Renewable and Sustainable Energy Reviews 184 (2023) 113589

Contents lists available at ScienceDirect

Renewable and Sustainable Energy Reviews

journal homepage: www.elsevier.com/locate/rser

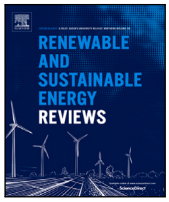

Review article

Wave devouring propulsion: An overview of flapping foil propulsion technology

Jingru Xing, Liang Yang *

Division of Energy and Sustainability, Cranfield University, Bedford, MK43 0AL, UK

ARTICLE INFO

Keywords:
Flapping foil
Wave devouring propulsion (WDP)
Hydrodynamics
Fluid–structure interaction
Hydrofoil
Wave-powered propulsion
Biomimetic thrusters

ABSTRACT

A comprehensive review of flapping foils for Wave Devouring Propulsion (WDP) is presented. The flapping foil can effectively utilize wave energy and generate thrust. The development of WDP is discussed, followed by an introduction to the geometry, modes of motion, and operating principles. These research studies are classified as theoretical, experimental, and numerical and are provided in detail. They demonstrate that marine equipment with a flapping foil system can achieve high energy conversion efficiency and low resistance. Several prototypes of the combination of WDP with human-crewed and uncrewed vessels have been shown, including the latest initial concept models and company products. There is a huge prospect for self-driven, pollution-free propulsion of marine devices, and this paper suggests several future studies.

1. Introduction

The ocean waves have a tremendous amount of energy. The flapping foil, as a wave propulsion device, can use the kinetic energy of the waves to achieve self-propulsion without fuel. This green propulsion technique converts wave energy into thrust using submerged flapping foils called Wave Devouring Propulsion (WDP). The human-crewed and uncrewed ships can be powered with WDP and achieve higher propulsion efficiency. The main purpose of this paper is to provide a comprehensive summary of the research on wave-induced flapping foils.

Flapping foils has been of great interest for a long time. The ability to generate thrust from surrounding flows was discovered and demonstrated as early as 1909. Knoller [1], and Betz [2] first explained the mechanism of thrust generation by a heaving foil in a uniform flow independently. The Knoller–Betz effect was verified experimentally by Katzmayr [3], who demonstrated that a foil could generate thrust in an oscillating flow and also assumed that this has the same effect as an oscillating foil in a uniform flow. For the uniform flow, McKinney and DeLaurier [4] tested the fluid as air instead of water. A windmill was analytically and experimentally investigated, which uses flapping airfoils to extract wind energy.

The phenomenon of propulsion is commonly observed in nature. The flight of birds and the forward movement of fish relies on the lift and thrust on their foil-shaped bodies. Lighthill [5] studied the biofluiddynamic behavior of aquatic animal propulsion modes, and concluded that the formation of the jet-like wake, also known as the reverse Von Karman vortex street [6], is an important phenomenon in the generation of thrust. This idea was subsequently confirmed by Koochesfahani et al. [7], Jones et al. [8], Buchholz et al. [9], Godoy–Diana et al. [10] and Lagopoulos et al. [11].

Flapping foils can also enhance traditional propulsion methods, which leads to the development of the wave devouring propulsion system (WDPS). It often utilizes a spring-loaded foil mounted under the bow or stern of the vessel. Early experiments by Jakobsen [12] and Terao [13] conducted the feasibility of wave powering ships. Subsequently, further research through experiments and numerical simulations have been conducted to deepen the understanding. Commercial products have been developed, such as the Wave Glider by Liquid Robotics [14], Autonomous Surface Vehicles by AutoNaut [15,16], and the M/F Teistin by Wavefoil, equipped with retractable bow foils [17].

In addition, WDPS operate at a lower frequency compared to traditional marine propellers, which can reduce the generation of underwater noise and its adverse effects on sea life, particularly marine mammals. Several numerical studies [18–22] used the acoustic wave equation Ffowcs Williams–Hawkings (FW-H) to understand the radiated noise levels. Belibassakis et al. [22] proposed that the hull geometry and acoustic properties of the vessel surface, as well as the effects of the sea surface and seabed, are crucial in determining the directionality of the generated noise.

The Fig. 1 illustrates the number of studies using theoretical, experimental and numerical approaches since 1954. This review aims to

* Corresponding author.
E-mail address: liang.yang@cranfield.ac.uk (L. Yang).

https://doi.org/10.1016/j.rser.2023.113589
Received 2 February 2023; Received in revised form 1 July 2023; Accepted 20 July 2023
Available online 29 July 2023

Nomenclature

ASV	Autonomous surface vehicle
AUV	Autonomous underwater vehicles
BDIM	Boundary data immersion method
BEM	Boundary element method
BIM	Boundary integral method
CAD	Computer-aided design
CFD	Computational fluid dynamics
DP	Dynamic positioning
EEDI	Energy efficiency design index
FAWPD	Floater-adjusted wave propulsion device
FLEUR	Flapping energy utilization and recovery
FSI	Fluid–structure interaction
FVM	Finite volume method
FW-H	Ffowcs Williams–Hawkings
GPU	Graphics processing unit
LCCA	Life cycle cost analysis
LE	Leading edge
NACA	National advisory committee for aeronautics
NSV	Natural-energy-driven surface vehicle
PV	Photovoltaics
RPM	Revolutions per minute
RvK	reversed von Kármán vortex street
SALL	Self-adjusting lower limit
SAWG	Single-body architecture wave glider
SST	Shear stress transport
TE	Trailing edge
TOMOT	Team of ocean mobile observation technology
UDF	User defined function
USV	Unmanned surface vehicle
vK	von Kármán vortex street
VOF	Volume of fraction
WAFT	Wave augmented foil technology
WDP	Wave devouring propulsion
WDPS	Wave devouring propulsion system
WEC	Wave energy converter
$\alpha_{eff}(t)$	Instantaneous effective AoA at time t
β	Ratio of the pitching frequency to the heaving frequency
$\Delta\theta$	Rotational deviation
ΔL	Extended length of the tension spring
Δy	Vertical deviation
λ	Wavelength
μ	Dynamic viscosity of the fluid
ω	Angular frequency
ϕ	Phase difference between the pitch and heave motion
ψ	Phase difference between wave and foil motion
ρ	Density of the surrounding flow
$\theta(t)$	Instantaneous angle formed between the oncoming flow and the chord at time t
θ_0	Pitch amplitude
(x_{TE}, y_{TE})	Location of the TE
$\dot{h}(t)$	Instantaneous heave velocity at time t
$\overline{C}$	Time-averaged coefficient
$\overline{F}$	Time-averaged force
$\partial D_B(t)$	Moving boundary to represent the flapping foil
∂D_F	Moving boundary to represent the free surface
∂D_W	Moving boundary to represent the vortex wake
A	Peak-to-peak oscillating amplitude of the foil's TE
c	Foil chord length
C_l	Lift coefficient
C_P	Power coefficient
C_t	Thrust coefficient
D	Foil thickness
f	Oscillating frequency
$F_h(t)$	Heave force
F_L	Lift force
f_n	Foil natural frequency
F_T	Thrust force
$f_{encounter}$	Encounter wave frequency
F_{ts}	Frequency ratio for torsional stiffness in pitching motion
$h(t)$	Instantaneous vertical displacement of the foil at time t
h_0	Heave amplitude
I	Foil inertia moment
k	Reduced frequency
K^*	Non-dimensional torsion stiffness
k_e	Pitch tension spring stiffness
K_h	Foil hydrostatic heave stiffness
k_h	Heave spring stiffness
K_p	Foil hydrostatic pitch stiffness
k_p	Pitch torsion spring stiffness
k_s	Parameter for adjusting waveform of perturbation signals
L_4	Arm length of the tension force
M_p	Pitch moment
$M_{pte}(t)$	Pitch tension moment
$M_{pto}(t)$	Pitch torsion moment
P	Pivot point
Re	Non-dimensional Reynolds numbers
s	Foil span
Sr_c	Chord-length-based Strouhal number

present a comprehensive summary of the existing research and industrial applications related to wave-powered foil propulsion and provide directions for future work in this field. The paper is structured as follows: In Section 1, we provide a brief introduction to foil propulsion and WDP technology. Section 2 delves into the key parameters related to foil study, including information on geometry, motion modes, and dimensionless parameters. The theoretical, experimental, and numerical researches on WDP are concluded in Sections 3, 4, and 5 respectively. Our aim is to provide an objective and comprehensive overview of the milestones and directions, focusing on wave-induced thrust efficiency, such as the degrees of freedom of the foil, the relative position of the foil to the attached body, and the free-surface effect, etc. In Section 6, we have conducted a comprehensive summary of the industrial development of WDP devices in table format, highlighting practical

Sr_D	Thickness-based Strouhal number
St_A	Amplitude-based Strouhal number
St_T	Path-length-based Strouhal number
T	Wave period
t	Time
T_{foil}	Trajectory length covered by the TE at the end of one oscillation period
u	Foil horizontal velocity
U_∞	Oncoming flow velocity
U_∞	Velocity of the characteristic flow
U_{wake}	Velocity of the wake
v	Foil vertical velocity

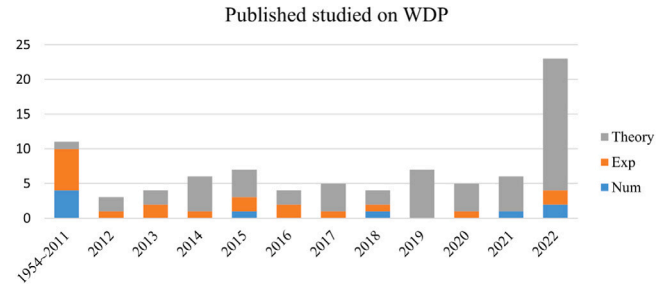

Fig. 1. The number of papers on WDP since 1954.

applications, products, and prototypes of foils and ships, foils and Unmanned surface vehicles (USVs), and foils and other connections. Finally, Section 7 suggest directions for future research.

2. Geometry and parameters

2.1. Foil geometry

The design and geometry of the flapping foils are crucial for the performance of WDPSs. One of the most commonly studied cross-sectional foil shapes is the NACA 4-digit foils, particularly the NACA0012 [23]. Other NACA models have also been used, such as NACA0015 [24–26]. Fig. 2 illustrates the characteristics of symmetrical and asymmetrical foils. The front and back ends of the wings are referred to as the leading edge (LE) and trailing edge (TE), respectively. The flat line joining LE and TE is known as the chord, and its length is denoted by c. The breadth of the foil is known as the span and is marked by s. The space between the upper and lower surfaces of the foil is known as the camber, and the line formed by the midpoint of their distance is known as the mean camber line. Additionally, it is noted that a foil cross-section does not necessarily have to be NACA-shaped, and a flat plate can also be considered a foil [27].

Only the wave-induced foil propulsion response is addressed in this paper. This type of foil is commonly referred to as "wave foil", "hydrofoil", "foil", "wing", "plate", etc. For the sake of convenience, they will be referred to collectively as "foil" in this paper.

2.2. Modes of motion

The flapping foils used in WDPSs have three modes of motion: heave, pitch, and flap. Heave motion refers to the vertical translation of the foil, pitch motion refers to rotation around a pivot point P, and flap motion is the result of a combination of heave and pitch motions, as illustrated in Fig. 3.

It is possible to constrain the movement of the foils in different ways. There are three types of movement of the foils: passive, semi-passive/semi-active, and active. In passive foils, the flapping motion is

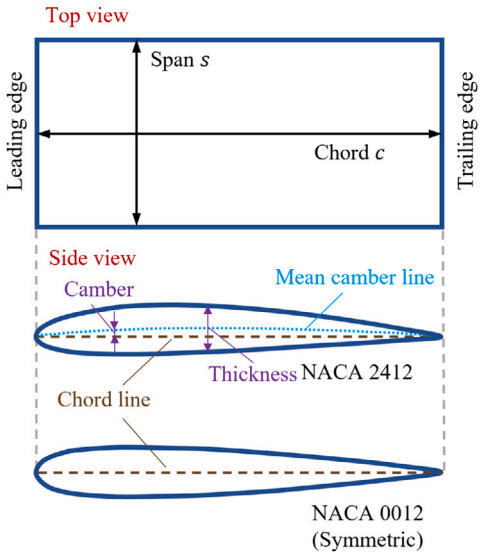

Fig. 2. The characteristics of the foil.

entirely flow-induced, and in most cases, these foils are accompanied by springs that provide restoring forces to ensure that the equilibrium position is restored. In semi-passive/semi-active foils, either heave or pitch is subject to a forced trajectory while the other motion is induced by the flow. In active foils, both heave and pitch motions are enforced, also known as "flap". Passive foils, while providing minimal disturbance to the flow, may not be as efficient as the semi-passive or active foils. Semi-passive foils, on the other hand, can achieve a balance between efficiency and minimal disturbance to the flow. Active foils, while being the most efficient, may introduce more disturbance to the flow. Therefore, the choice of the type of movement and the control of the relative parameters will depend on the specific objectives.

For the passive foil, there have been several studies exploring the use of elastically deformed flapping foil propulsion. These works primarily focused on the chordwise deformation of the flapping foil, as demonstrated in studies by Anevlavi et al. [28] and Fernandez–Prats [29], among others. Additionally, Zhu [30] investigated the influence of spanwise flexibility, providing insights into the behavior of the system when spanwise deformation is considered. By examining the impact of both chordwise and spanwise flexibility, these studies contribute to a deeper understanding of the potential benefits and challenges associated with incorporating flexible foils in WDP systems.

However, it is worth noting that in most cases, passive foils are rigid foils accompanied by springs. The inclusion of springs allows for the provision of restoring forces, ensuring that the foils return to their equilibrium positions. Eq. (1) provides a general representation of the instantaneous heave force and pitch moment applied to the foil. Researchers can also experiment with different types of springs, such as torsion springs or tension springs, to achieve optimal results.

$$F_h(t) = k_h \Delta y \tag{1a}$$

$$M_{pte}(t) = k_p \Delta\theta \tag{1b}$$

$$M_{pto}(t) = k_e \Delta L L_4 \tag{1c}$$

where, $F_h(t)$ is the heave force, $M_{pte}(t)$ is the pitch tension moment and $M_{pto}(t)$ is the pitch torsion moment. k_h, k_p and k_e are the heave spring stiffness, pitch torsion spring stiffness and pitch tension spring stiffness. Fig. 4 illustrates two different pitch springs, a torsion spring and a tension spring. Δy and $\Delta\theta$ are the vertical and rotational deviation of the foil from its initial position at time t, respectively. ΔL is the extended length of the tension spring, and L_4 is the arm length of the tension force.

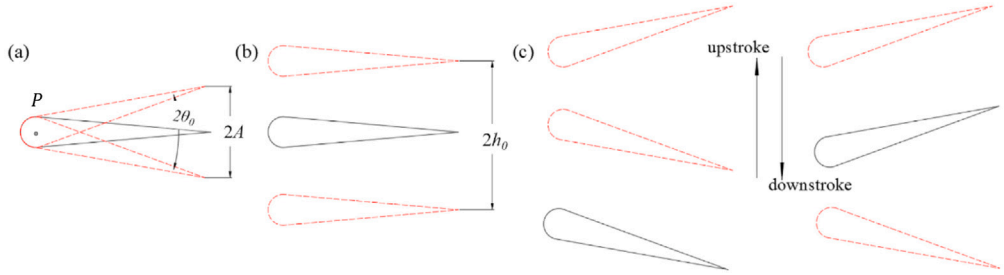

Fig. 3. The motions of foil: (a) pitching motion, (b) heaving motion and (c) flapping motion of a foil (Wu et al. [23]).

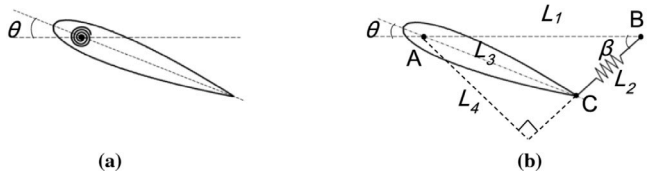

Fig. 4. (a) torsion spring, (b) tension spring (Feng et al. [31]).

The semi-passive and active foils have prescribed trajectories for the heave and pitch motions. This is achieved by setting harmonic motion for both the heave and pitch, as described in the equations (Eq. (2a)) and (Eq. (2b)).

$$h(t) = h_0 \sin(\omega t) \tag{2a}$$

$$\theta(t) = \theta_0 \sin(\omega t + \phi) \tag{2b}$$

where $h(t)$ is the instantaneous vertical displacement of the foil. $\theta(t)$ is the instantaneous angle formed between the oncoming flow and the chord, also referred to as the angle of rotation. h_0 and θ_0 is the heave and pitch amplitude. ω is the angular frequency (rad/sec), equal to $2\pi f$, where f is the oscillating frequency, and ϕ is the phase difference between the pitch and heave motion. ϕ is an important parameter to consider, as it can impact propulsion efficiency. Platzer et al. [32], and Pedro et al. [33] suggested $\phi = 90°$ in uniform flow as the optimal phase difference between pitch and heave. De Silva and Yamaguchi [34] suggested that the optimal phase difference between wave and foil motion (ψ) = −90° (among −180° and +180°) while the optimal phase difference between heaving and pitching motion (ϕ) = 60° (among 0° and +180°) in wavy flow.

Various perturbation signals can be added to the basic sinusoidal signal in Eq. (2a) for active heaving motion in order to achieve a broader variety of active heaving motion patterns [35,36]. By adjusting the parameter k_s, perturbation signals with different waveform cycle trajectories, including sawtooth, sine, and square, can be generated. Increasing k_s leads to a change in the heaving perturbation signal from a sawtooth to a sine wave, and finally to a square wave (Fig. 5(a)). Apart from heave signal, Qi et al. [37] considered different waveform for pitching motion signal by adjusting β (Fig. 5(b)). β is defined as the ratio of the pitching frequency f_p to the heaving frequency f_h, i.e. $\beta = f_p/f_h$. When β increases, the pitching profile of the oscillating foil tends from sinusoidal to trapezoidal.

For foils subject to an oncoming flow, the resulting angle of attack (AoA) is related to the heave velocity, and pitch angle as illustrated in Fig. 6 and expressed from Eq. (3) [23,38,39].

$$\alpha_{eff}(t) = \theta(t) - \arctan\left(\frac{\dot{h}(t)}{U_\infty}\right) \tag{3}$$

where $\alpha_{eff}(t)$ and $\theta(t)$ is the instantaneous effective AoA and pitch angle and $\dot{h}(t) = \frac{dh}{dt}$ is the instantaneous heave velocity.

During such harmonic motions, foil undulations generate wake patterns that result in either drag or thrust. The foil enters a drag-dominated state when a von Kármán vortex street develops (vK) [6], because the flow velocity in the wake falls below the ambient/oncoming velocity. An equal flow velocity in the wake occurs when the vortex at the foil's trailing edge aligns, resulting in a neutral flow state at the foil. When a reversed von Kármán vortex street develops (RvK), the foil experiences thrust due to the higher velocity of the flow in the wake than the ambient/oncoming flow. This drag-to-thrust wake transition stage has been extensively studied for flapping foils in uniform flows, and the foil transition towards thrust occurs with a delay relative to the drag-to-thrust wake transition stage [11,40–42]. Fig. 7 illustrates three fundamental wake patterns, where U_{wake} is the velocity of the wake and U_∞ is the characteristic flow velocity.

2.3. Dimensionless parameters

Foils that interact with viscous forces experience thrust, drag and lift forces. Previously, we discussed how the formation of an RvK vortex street is linked to the transition from drag to thrust wakes. Upon exceeding the ambient flow velocity, thrust jets are produced, causing the foil to experience a thrust force — total force acting on the x axis (usually horizontal axis) [11,43,44]. Lift and thrust forces are generally expressed as dimensionless lift (C_l) and thrust coefficients (C_t). These coefficients are calculated by normalizing the force acting on the foil with the dynamic pressure of the oncoming flow at platform area of the foil, as shown in Eq. (4). Moreover, the power coefficient (C_P) can be present using an analogue expression [45].

$$C_l = \frac{F_L}{\frac{1}{2}\rho U_\infty^2 cs} \tag{4a}$$

$$C_t = \frac{F_T}{\frac{1}{2}\rho U_\infty^2 cs} \tag{4b}$$

$$C_P = \frac{P}{\frac{1}{2}\rho U_\infty^2 cs} \tag{4c}$$

where, ρ is the density of the surrounding flow. F_L and F_T is the lift and thrust force, c is the foil chord and s is the foil span. P is the power and can be calculated by the vertical velocities ($\frac{dh}{dt}$) and angular velocities ($\frac{d\theta}{dt}$), i.e. $P = -F_L\frac{dh}{dt} - M_p\frac{d\theta}{dt}$, where M_p is pitch moment. In addition, Eq. (4) refers to instantaneous coefficient values and the time-averaged, e.g. over one wave period T, forces and coefficients ($\overline{F_L}$ and $\overline{C}$) are calculated as:

$$\overline{C} = \frac{1}{T}\int_0^T C(t)\mathrm{d}t \tag{5}$$

$$\overline{F_T} = \frac{1}{T}\int_0^T F_T(t)\mathrm{d}t \tag{6}$$

$$\overline{F_L} = \frac{1}{T}\int_0^T F_L(t)\mathrm{d}t \tag{7}$$

where, $\overline{C}$ can be any of $\overline{C_l}$, $\overline{C_t}$, $\overline{C_t}$ and $\overline{C_P}$.

The interaction between a moving foil and the oncoming flow is described through the non-dimensional Reynolds and Strouhal numbers. The chord based Re is calculated from Eq. (8a), while several expressions for the Strouhal number have been proposed. Two elements in the foil oscillation affect the wake pattern: the peak-to-peak oscillating

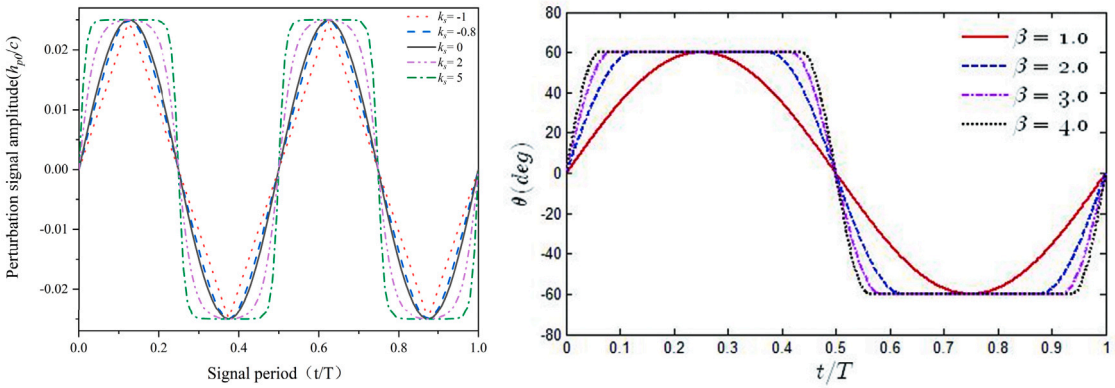

(a) Variation of the perturbation signal waveform in one period at different k_s. (Gao et al. [36])
(b) Time variation of $\theta(t)$ for different values of β in one period. (Qi et al. [37])

Fig. 5. Non-sinusoidal heaving and pitching motion signal.

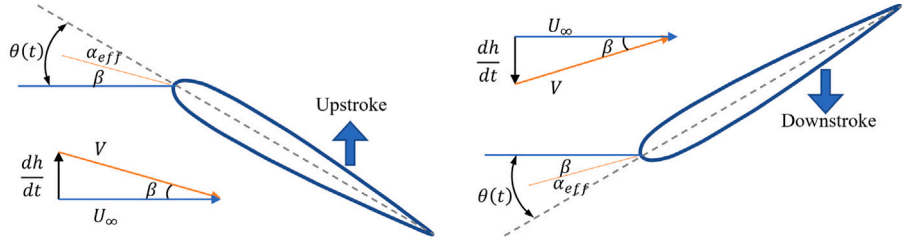

(a) Upstroke (b) Downstroke

Fig. 6. The illustration for the effective AoA α_{eff} of flapping foil in uniform flow ($\frac{dh}{dt}$ is the heave velocity, V is the velocity of the stream relative to the foil.).

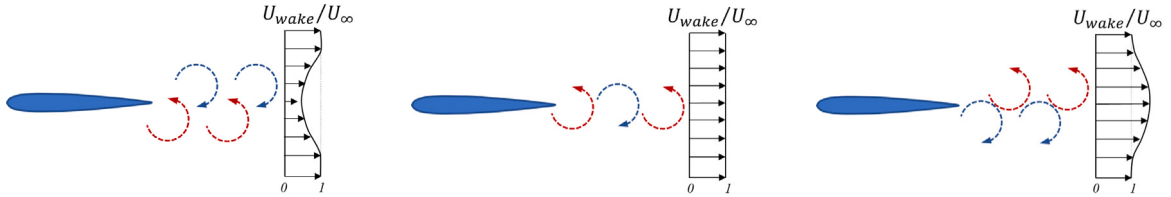

(a) vK street (b) Neutral regime (c) RvK street

Fig. 7. The illustration for the drag-to-thrust wake transition of flapping foil.

amplitude, A, of the foil's trailing edge and its oscillating frequency, f. The current mostly used Strouhal number combines both, St_A, Eq. (8b) [46]. To be dimensionless, the former element is normalized by the thickness D or chord length c to $A_D = A/D$ or $A_c = A/c$ and the latter becomes reduced frequency k, $k = U_\infty/fc$. Based on the reduced frequency, a thickness-based Strouhal number $Sr_D = fD/U_\infty$ and a chord-length-based Strouhal number $Sr_c = fc/U_\infty$ also have been proposed by Godoy–Diana et al. [10] and Cleaver et al. [47], but St_A is often preferred to better characterize the wake pattern, i.e. RvK street, with a single factor. Recently, a path-length-based Strouhal number Eq. (8c) was proposed by Lagopoulos et al. [11], which should be higher than 1 in order for the foil to produce thrust. In contrast, Read et al. [38] reported optimum thrust generation for $0.2 < St_A < 0.4$.

$$Re = \frac{\rho c U_\infty}{\mu} \tag{8a}$$

$$St_A = \frac{fA}{U_\infty} \tag{8b}$$

$$St_T = \frac{fT_{foil}}{U_\infty} \tag{8c}$$

$$T_{foil} = \int_0^T \sqrt{u(x_{TE}, y_{TE}, t)^2 + v(x_{TE}, y_{TE}, t)^2}\,dt \tag{8d}$$

where ρ is the density of the surrounding fluid, μ is the dynamic viscosity of the fluid. T_{foil} is the trajectory length covered by the TE at the end of one oscillation period. u is horizontal velocity of the foil and v is vertical velocity of the foil. The (x_{TE}, y_{TE}) in the Eq. (8d) is the location of the TE. For forced harmonic oscillating motions, $2h_0$ is an estimate for the width of the foil wake. Thus A can be approximated with $2h_0$, and since $f = \frac{\omega}{2\pi}$ Eq. (8b) is also written as Eq. (9).

$$St_A = \frac{\omega h_0}{\pi U_\infty} \tag{9}$$

Zurman–Nasution et al. [48] investigated the limitations of using 2D simulations to study 3D flapping foil motion through the boundary data immersion method (BDIM) and suggested that the valid two-dimensional simulation lies in the St_A range of 0.15 to 0.45.

Non-dimensional parameters are introduced to represent spring stiffness when the foil is restricted by spring force. Yang et al. [49] proposed a non-dimensional parameter frequency ratio (F_{ts}) for torsional stiffness in pitching motion, which is expressed in Eq. (10a).

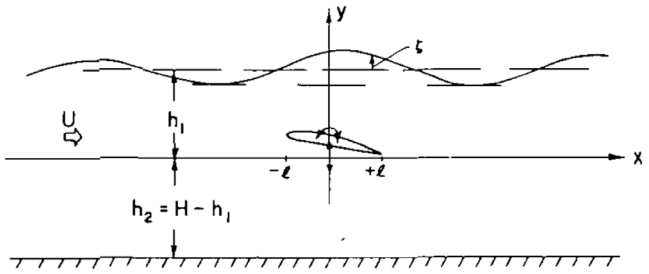

Fig. 8. Body coordinate system for a two-dimensional foil heaving and pitching in a regular water wave (Wu et al. [55]).

Similar to the equation defining the coefficient in Eq. (4), Thaweewat et al. [50] and Zhang et al. [51] and Chen et al. [52] proposed a non-dimensional torsion stiffness (K^*), see Eq. (10b). In Xing et al. [53]'s study, the spring stiffness was normalized directly using the foil hydrostatic stiffness (K_h and K_p) in calm water, i.e. k_h/K_h and k_p/K_p as non-dimensional heave and pitch spring stiffness.

$$F_{ts} = \frac{f_n}{f_{encounter}} \tag{10a}$$

$$K^* = \frac{k_p}{\frac{1}{2}\rho U_\infty^2 cs} \tag{10b}$$

where f_n is the foil natural frequency and defined as $f_n = \sqrt{k_p/I}/2\pi$. I is the inertia moment of the foil. $f_{encounter}$ is the encounter wave frequency.

3. Theoretical study in WDP

3.1. Introduction of the WDP concept

The concept of WDP, or Wave Devouring Propulsion, was first proposed in the 1950s by Weinblum and Georg [54] who proposed a theoretical method for studying the seaworthiness of foils. They calculated the hydrodynamic forces of heaving or pitching foil systems without a hull in regular waves of small amplitude by theory with the result that the simplification did not involve severe errors in the cases considered.

Inspired by Weinblum and Georg's work, Wu et al. [55] found that oscillating foils could extract energy from the waves. They suggested that energy can only be extracted when the waves have a vertical velocity component to both the mean free stream and the span of the flapping foil (Fig. 8). However, this study [55] ignored boundary effects, i.e. they placed the foil more than two chords away from each boundary and did not consider the effects of the free water surface and the solid bottom.

Isshiki [56] extended Wu's theory by theoretically proving the possibility of thrust generation by a passive flapping foil in waves while taking into account the effect of the free surface. In fact, according to recent studies [56–59], free surface effects should always be taken into account as the free surface strongly influences the vortex wake and the forces upon the foil. The effect of the free surface is only minor (below 2%) when the foil is submerged in the unbounded domain for more than 1.71 chord lengths [60].

Isshiki [56]'s study is also the first time the term 'Wave Devouring Propulsion (WDP)' has been introduced to summarize the fact that wave energy can be transformed by flapping foil to thrust generation. Isshiki then conducted a series of experimental studies on WDP in the following years, which will be continued in Section 4. Based on the experiment of the SR108 ship model in [61], Isshiki [62] roughly estimated the propulsive performance of HandyMax B/C under Beaufort 10 with the same boat length in [61] and pointed out that there was no need to extract foil out of the calm sea when running because the benefit gained in bad weather can compensate for the increased resistance of the boat in calm seas due to the foil.

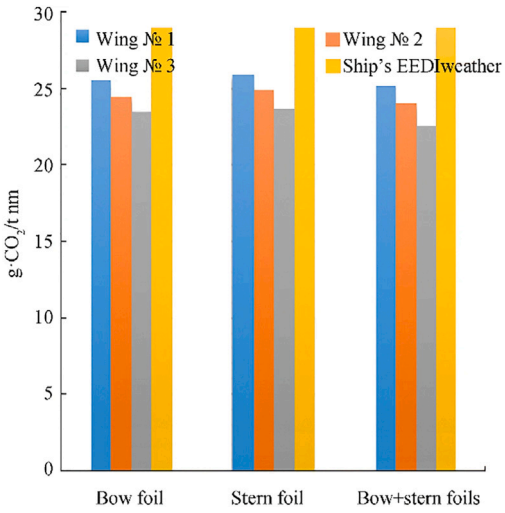

Fig. 9. Results $EEDI_{weather}$ of a container ship S-175 with wing devices at a representative sea condition (Ship speed = 22 kn) (Rozhdestvensky et al. [65]).

3.2. Mathematical models

The mathematical models proposed to better understand the physics of WDP and to use it as an engineering tool in the marine field include those developed by Grue et al. [58], which used a vortex distribution along the centerline of the foil and the wake under infinite water depth, and resulted in good agreement with experimental results of Isshiki et al. [63]. Lopes et al. [64] proposed an analytical model to better understand the physics of WDP, and after validation, it was shown to capture oscillating foil lift and thrust forces with enough precision, but does not consider the presence of a free surface. Rozhdestvensky et al. [65] presented a mathematical model of a ship with foil devices on the bow or stern and found that the ship in head seas had reduced heave and pitch motions, especially when the foil was attached to the bow. They also noted that the energy efficiency design index (EEDI) for ships with foils was lower than those without foils, reflecting a reduction in CO2 emissions due to fuel consumption in representative sea conditions, see in Fig. 9. Bowker et al. [66] proposed a prediction method that shows the ship's length influences the efficiency of bow foils in various regions of the world, with the optimum conditions for efficient bow foil operation being waves with an average encountered wavelength similar to the ship's length. Rozhdestvensky [67] conducted a parametric analysis on underwater gliders and wave gliders using simplified mathematical models, and the wave gliders model can assess the effect of wave parameters, foil size, and shape on the efficiency of wave-induced thrust generation.

4. Experimental study in WDP

4.1. Experiments on foil itself

The foil is the physical mechanism that allows WDP to take place. Several researchers and groups have focused on the foil itself, as well as innovative deformations of the foil and their hydrodynamic response under different wave conditions.

Isshiki et al. [63,68] conducted a series of experiments and theoretical discussions about the WDP of a foil placed in waves with a shallow draft. The heaving and pitching motions of the foil were restricted by springs, and the results showed that as the wavelength increases, the passive foil's forward speed and heave amplitude tend to rise in short waves and fall in long waves. Their theoretical calculations also showed a higher forward speed for a deeper draft, which was later confirmed

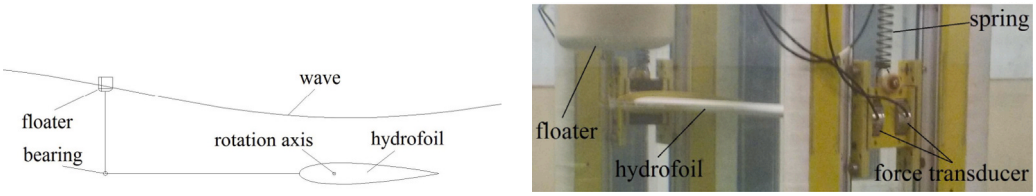

(a) The sketch map of FAWPD (b) A closer look at the setup

Fig. 10. FAWPD setup (Hao et al. [69]).

by the experimental work of Hao et al. [69]. These early studies were important for later analysis of numerical WDP [34,58,59,70].

Hao et al. [69] proposed an innovation in wave propulsion devices by adding small floaters to adjust the pitch motion of the foil, named the floater-adjusted wave propulsion device (FAWPD) (Fig. 10). They compared the FAWPD to a passive foil and found that when the wave-chord ratio is greater than 15, the average thrust of the FAWPD is significantly greater than that of the passive foil for the same wave conditions. This semi-active foil allowed for greater thrust in deeper submergence, in contrast to the behavior of a sole passive foil. Wang et al. [71] tested the dynamic response of a fully passive foil under wave condition.

4.2. Experiments on WDP ship

In the early stages of WDP research, researchers were optimistic and ambitious in their expectations about the capabilities of the WDP. In 1981, Jakobsen [72] experimentally studied the movement of a ship model with foils against waves. Jakobsen's 1 m model was proved to move about 1 m/s under waves (wavelength=2.25 m, wave height =0.1 m). Jakobsen [12] also experimented with full-size models but in a controlled environment and showed that if the energy of the waves is sufficient, the WDP produced ship speed could reach or even exceed the speed produced by the ship's conventional propulsion system. Terao [13] tested a floating body with foils on the fore and aft and the model moved toward the waves without any propelling power or control systems. Isshiki [73] suggested that the ship with flapping bow foil can be driven solely by wave power under certain conditions.

The use of foils for ship propulsion has gained attention in recent years, as research has demonstrated the positive effects of foils on ship performance. However, questions about the optimal number and placement of foils on ships have yet to be fully answered. Research has focused on the use of bow foils, which are foils attached to the bow of a ship. Studies have been conducted using both model ships and actual vessels. Isshiki and Murakami [61] conducted a free-running test of a 2 m long SR108 container ship model with rigid foil fixed to the bow under waves. They found that when the wavelength is about 1 m, which is half of the ship model length, the pitch of the ship model becomes prominent, and the ship model runs very fast. Using the same ship model in [61], Isshiki and Naito [74] conducted towing tests and theoretical calculations on the ship resistance and found the calculated results are slightly higher than the experimental ones while having a similar tendency. Turning to the actual sea state, the tests of a 15.7 m long fishing boat with bow foil were conducted by Isshiki et al. [75]. The theory overestimated the effects of the foil as in [74], but the theory explained the experimental results qualitatively. Bøckmann and Steen [76] conducted a model test of a 1:16 scale model ship with fixed a foil bow (Fig. 11) in regular head waves with 3.7 m wave height and 8.6 s period. The results showed that when the ship's speed was 12 knots, the fixed foil resulted in a 60%, 42% and 45% reduction in ship resistance, heave and pitch motions. Bowker and Townsend [77] evaluated the bow foil effect on a generic cargo ship in waves and showed that the passive spring-loaded bow foil (Fig. 12) reduces an average ship pitch and heave by 20% and 10% respectively, and the delivered power by up to 50% in regular head waves and estimated by 12% in irregular waves.

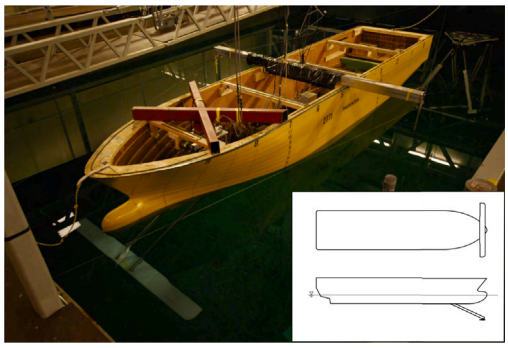

Fig. 11. 1:16 scale model ship with a fixed foil bow (Bøckmann and Steen [76]).

Instead of one foil, two foils at the bow can show a similar reduction effect even with different ship types and wave conditions. Feng et al. [78] studied the hydrodynamic performance of a container ship with a pair of foils fixed at the bow under head sea conditions. They developed a frequency domain model and conducted a model experiment in the towing tank, which proved theoretically and experimentally that 80% reduced the peak response, 30% and 25% for added resistance, heave and pitch, compared to the original hull. Long-term prediction of 3100TEU container ship at actual seas was also conducted and showed a slight reduction in EEDI of this ship while the WDPS predicted to be effective in all the sea areas along the sailing route. Bøckmann et al. [25] conducted the model test and time-domain simulation on a tanker ship with two foils, called Wave Augmented Foil Technology (WAFT). The foils are fixed on the bow of the hull, see Fig. 13. They found that the implementation of wavefoils has lowered the full-scale resistance of the ship by 9%–17% in typical sea conditions. In the experiments of Huang et al. [79] a 1:50 scale model of a container ship was used for free running tests with fixed propeller speed (714 Revolutions per minute (RPM)). The effects of two fixed and active pitch-oscillating of the bow foils were compared. The results show that in regular waves, the speed improvement is up to 6.24% (0.864 m/s when fixed) for a wavelength to boat length ratio of 1.0 and 11.86% (0.882 m/s when fixed) for a ratio of 1.3. Terao [80] carried out model tests (Fig. 14) for the Suntory Mermaid II – a wave-powered boat – as the experimental support of this CO2-free vessel and summarized the relevant data from its voyage. For the WDPS design of this vessel, two foils were installed in tandem connection on the bow of this catamaran model and soft springs provided each foil's pitch restoring force to move individually.

The placement of foils on ships has not only been limited to the bow, but researchers have also explored the potential of foils placed on the stern. McGregor and Thomson [81] conducted full-scale sea trials on a 6 m long Caprice yacht with a foil mounted on the stern and found that the flexible foil propeller could convert wave energy into forward motion, acting as an aid to the yacht's movement. The use of foils on both the bow and stern of a ship has also been studied by researchers

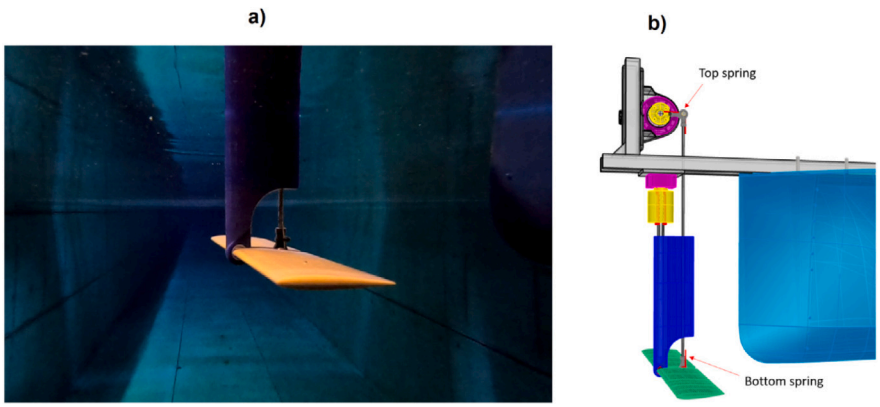

Fig. 12. Neutrally buoyant, spring loaded foil mounted to the bow of the model (a) Underwater image (b) Computer-aided design (CAD) rendering (Bowker and Townsend [77]).

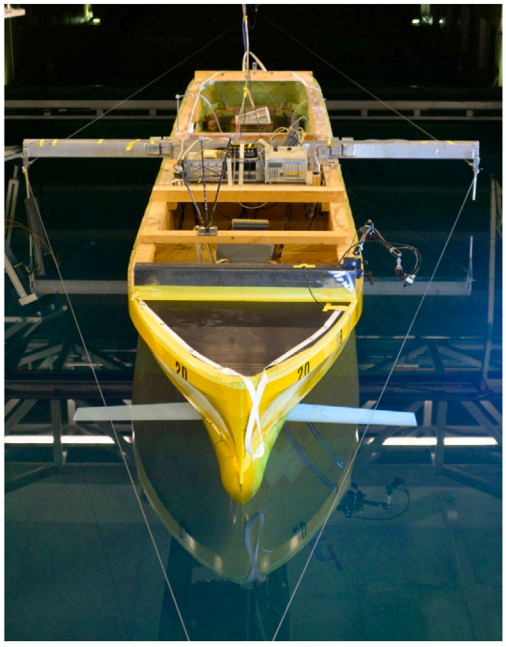

Fig. 13. The tanker ship model with two fixed foils (Bøckmann et al. [25]).

Fig. 14. Test model of Suntory Mermaid II equipped with all sensors and WDPS (Terao [80]).

such as Bowker's team [82,83]. Bowker et al. [82] investigated the performance of an Autonomous Surface Vehicle (ASV) equipped with two passive foils submerged at the bow and stern in head waves in a towing tank, and named this WDPS device Flapping Energy Utilization and Recovery (FLEUR) system, see Fig. 15. They found that the FLEUR device can provide propulsion or power generation for the ASV, with an attainable output of 4 watts and an average of 1 watt. Using the same FLEUR prototype, Bowker et al. [83] presented a discrete time-domain numerical model that was validated with the experimental results, and showed the dominance of the forward foil over the aft foil in the propulsion effect.

4.3. Experiments on other WDP structures

Offshore energy is an emerging technology in the marine field, which might benefit from WDP for resistance reduction and floating structure stabilization. Terao and Sakagami [84] proposed two new applications of WDPS—floating wind turbine generator systems placed on the catamaran with a foil installed under the bow of the hull and another one based on an active control system. They suggested the WDPS can reduce the wave drift forces and pitching motion in waves. Without using any ship to apply WDPS, Yoshida et al. [27] directly connected the foil with a platform and presented the applicability of WDP for a floating platform. Three flat plate-type foils were horizontally attached to the lower beams of the semi-submersible model, see Fig. 16. They studied the effects of the foil thickness, foil draft, wave directions, wavelength and attached foil directions and showed the top-view trajectory under different tests. Their research confirmed using a foil attached to a floating body to support the dynamic positioning (DP) system with less energy consumption.

4.4. Brief discussion of experimental result

The experimental studies on WDP have shown promising results in terms of reducing ship resistance and response magnitude during rough waves. The majority of the experiments were conducted in regular head waves and it has been found that the foils are more effective when attached to the bow rather than the stern. Researchers have primarily focused on fixed, passive, and semi-passive foils, the selection of which depends on the needs of the WDPS device. The results of these experiments have demonstrated that the WDP characteristics of the foil can not only be used as an auxiliary means of propulsion but also as a stabilizer on vessels and floating structures. Overall, the potential for utilizing WDPS in marine transportation and other industries is significant and further research is needed to fully realize its potential.

5. Numerical study in WDP

In this section, we discuss the numerical studies on WDP, which can be divided into two groups of numerical solver, potential flow theory and viscous Navier–Stokes solver. Both approaches are widely used in the WDP research, and we will present their advantages and limitations.

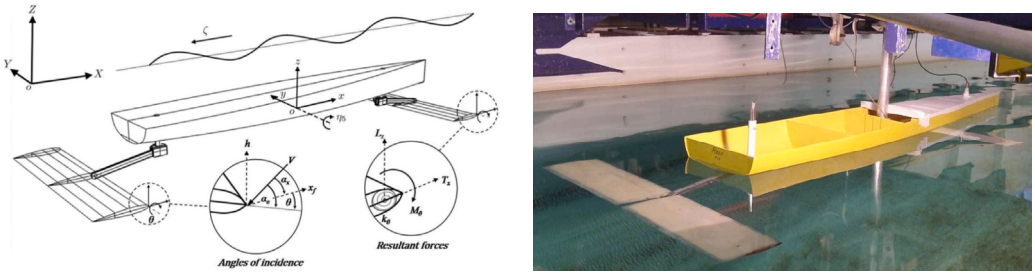

(a) Frames of reference (b) Carriage setup of FLEUR

Fig. 15. FLEUR (Bowker et al. [82,83]).

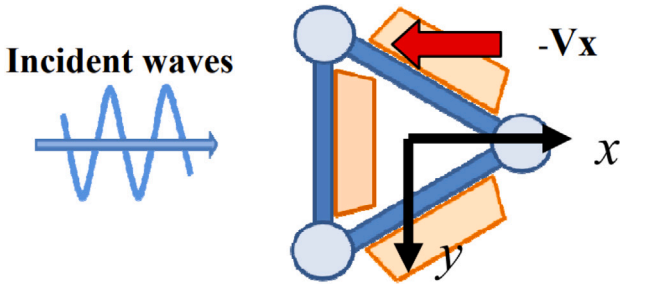

Fig. 16. Incident wave angle and attached wing direction in the basic performance test of floating structure (Yoshida et al. [27]).

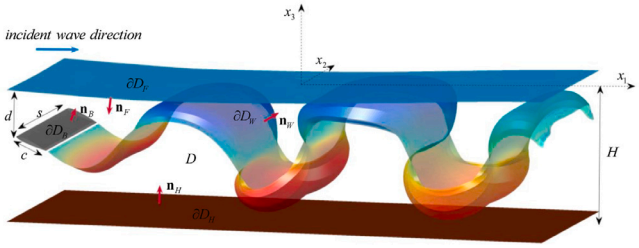

Fig. 17. Definition of the wave flapping foil problem in the case of a foil (of chord c and span s) in flapping motion under the free surface (at mean submergence d) and in head waves over bathymetry with constant depth H (Filippas and Belibassakis [85]).

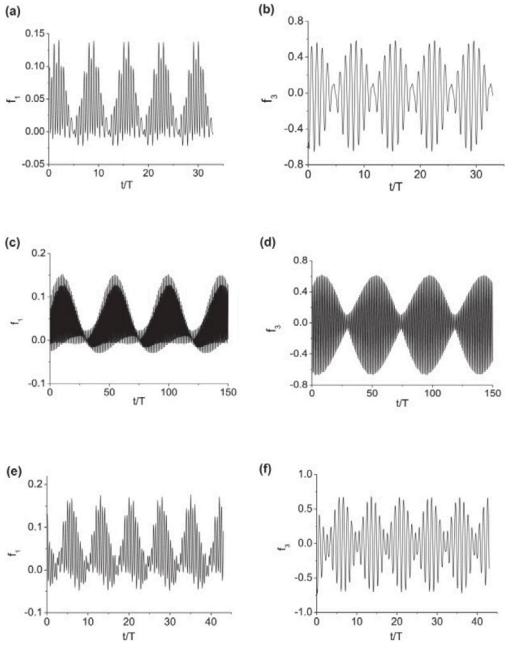

Fig. 18. The time history of the foil with (Xu et al. [86]).

5.1. Potential flow solver

Boundary Element Methods (BEM), also known as Panel Methods or Boundary Integral Methods (BIM), is a widely used numerical simulation tool for studying active foil wave propulsion since 2012. BEM is based on the potential flow theory, which assumes that the fluid is an ideal fluid, and therefore viscosity is not taken into account in the simulation. BEM is used to solve boundary value problems by representing the fluid–structure interaction as a time-dependent problem. The flapping foil is represented by a moving boundary $\partial D_B(t)$ in an earth-fixed reference frame. The free surface and vortex wake are represented by ∂D_F and ∂D_W, respectively. A pressure-type Kutta condition is applied on the trailing edge of the foil to model the vorticity shed by the foil. The hydrodynamic forces and moments on the foil can be directly obtained by instantaneous pressure integration over the body surface (see Fig. 17).

Studies using the BEM method have involved both 2D and 3D simulations of flapping foil. Filippas et al. [59,87] analyzed active flapping foils operating under free surfaces and in waves using the unsteady 2D developed-BEM and compared them with experimental results. Due to the development of wave resistance associated with the generation of the complex wave system, at the same pitch maximum angle, the infinite field C_t is maximum. When the submergence/chord is less than 2.5, the closer to the free surface, the lower the C_t. Xu et al. [86] studied the active flapping foil in fifth-order Stokes waves of infinite water depth and the effects of the frequency difference between foil motion and waves. Fig. 18 showed that when the frequency of the foil motion is close to the encountered wave frequency, clear envelopes of the force curves can be found, which means the foil's pitch varies violently. The force amplitude varies considerably for each period in Fig. 18, indicating that the local flow velocity and the effective AoA of the foil differ substantially during the different oscillations. Also, the free surface effect becomes less significant with increasing heave amplitude and pitch angle [86]. One notable work in the field of 3D BEM is by Belibassakis and Politis [88], which focuses on the hydrodynamic performance of flapping wings for enhancing ship propulsion in wave conditions through active control. They investigated two configurations: horizontal and vertical flapping wings positioned beneath the ship's hull. The findings revealed that both vertical and horizontal flapping wings contribute to thrust production, ranging from 10% to 50% of the ship's calm-water resistance at the same speed. Notably, their present system enhanced the ship's propulsive performance while providing significant dynamic stabilization, particularly in the case of the horizontal flapping wing. Building upon this work, Belibassakis and Filippas [89] further explore the interconnected dynamics between hull motion and a horizontal flapping foil positioned below the keel in the presence of an irregular head wave associated with specific sea conditions. They found that when the wave height increased significantly,

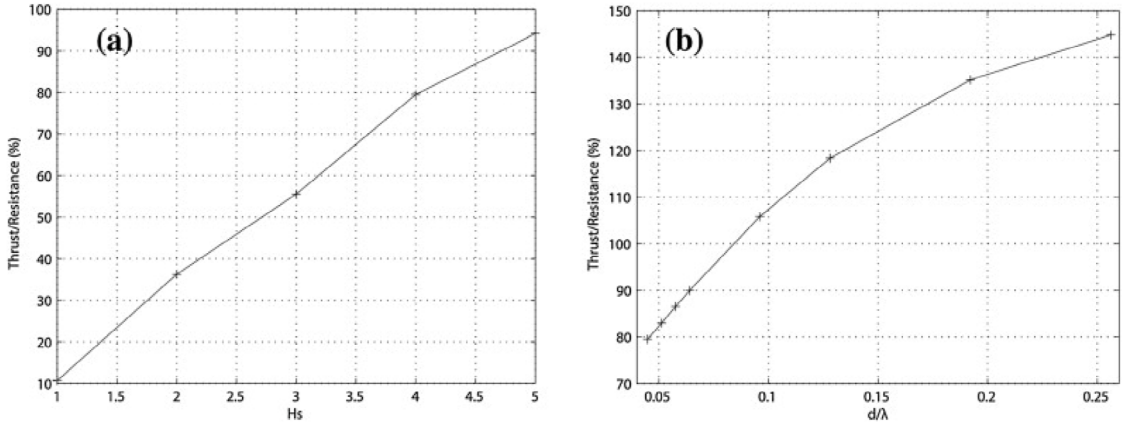

Fig. 19. Mean thrust to calm water resistance ratio as (a) function of sea conditions represented by significant wave height, and (b) as function of the mean foil submergence to modal wavelength ratio (Belibassakis and Filippas [89]).

more thrust could be produced (see Fig. 19(a)). Moreover, Fig. 19(b) indicated a decrease in thrust/resistance ratios at lower submergence. According to Isshiki et al. [68], the decrease of the draft results in increased thrust, which is acceptable as lower submergence means more wave energy that can be transformed into thrust. However, lower submergence also means more wave resistance due to the effect of the free surface. In addition, the vertical oscillating motion of the foil caused by the vessel's pitching is reduced due to the smaller radius of rotation. Thus, it is suggested in this case that the growth of thrust does not exceed the growth of resistance because of the significant wave resistance from the attached ship. Furthermore, it brings to our attention that when the size of the boat is too large to a certain extent, the submergence depth of the foil should not be too shallow. In practice, the optimum submergence depth of the foil should be chosen in relation to the size of the boat for higher propulsion efficiency. Recently, there have been advancements in utilizing graphics processing units (GPUs) for research purposes. Filippas and Belibassakis [85] introduced the use of GPUs for time-domain BEM analysis, specifically focusing on the hydrodynamic performance of 3D submerged flapping foils, also known as biomimetic thrusters. Their work demonstrated that employing GPUs in mixed precision instances resulted in superior computational speed without significant compromise in accuracy.

5.2. Navier–Stokes flow solver

Computational fluid dynamics (CFD) solves Navier–Stokes equations with suitable turbulence models. It extends the applicability of potential flow theory by taking into account the effects of viscosity. In Table 1, a chronological overview of previous CFD studies on WDP is presented, revealing distinct research objectives that can be broadly categorized into four main application areas: wave-propelled physical mechanisms, ASV, ship propulsion, and other innovative marine systems.

A comprehensive understanding of the underlying physical mechanisms is essential for its widespread application in marine vehicles and platforms. These studies typically focus on the movement of foils and employ CFD simulations to explore a wide range of conditions that cannot be easily achieved through experimental means. For instance, Gao et al. [36] studied different perturbation signal based on sinusoidal heave waveforms by adjustable parameter k_s such as sawtooth ($k_s = -1$), sine ($k_s = 0$), and square ($k_s = 5$), mentioned in Fig. 5(a). Gao et al. [36] investigated fluid dynamics around the heaving foil with finite volume method (FVM) and found that adding any waveform perturbation increased the axial thrust. As the perturbation frequency increases, all wake structures first go through an asymmetric wake phase (at perturbation frequency = 2 Hz) and finally evolve into a chaotic wake. While Gao et al. [36] focused on the heave waveforms, Qi et al. [37] studied active oscillating foils with sinusoidal and non-sinusoidal pitch (Fig. 5(b)) using the dynamic and moving mesh. For the sinusoidal pitching ($\beta = 1$), as the reduced frequency increased, both the mean output power coefficient and the optimal pitching amplitude increased. For the non-sinusoidal pitching, when the pitching amplitude was small, as β increases, the propulsive performance of the flapping foil gradually improves, with the trapezoidal-like pitching profile ($\beta = 4$) being more effective. De Silva and Yamaguchi [34] investigated the active 2D oscillation foil in wavy flow for marine propulsion by using the custom Fluent solver with the dynamic mesh technology and the Volume of Fraction (VOF) method. They suggested when the ratio of wave amplitude to foil chord length is between 1/14 and 3/14, over 50% of the wave energy can be converted into propulsion energy. In recent years, the utilization of foils in ASVs has garnered significant attention due to advancements in technology. Researchers are increasingly recognizing the immense potential of foils, particularly in the form of wave gliders, for various ASV applications. A notable characteristic of wave glider simulations is the omission of the free surface. This omission is justified by the fact that the hydrofoil is typically submerged under the surface by more than four times its chord length [95]. Consequently, the influence of the free surface can be considered negligible, allowing the domain to be treated as an infinite fluid without incorporating the ship and the free surface in the simulation. Yang et al. [105] predict the dynamic performance of the wave glider with six pairs of 3D tandem foils in head seas. The interaction of flow and the boat-foil system was simulated by FINE/Marine with VOF model and the passive eccentric rotation of foils was simulated by STAR-CCM+ with overset mesh. The passive rotation was restricted by the spring force that restore them to the original position. Fig. 20 was the vortex structure of the six tandem foils in one cycle. Foils rotated counterclockwise as the glider descends (a-e), clockwise as the glider ascends (f-g). In addition, when the glider was in a trough, the clockwise rotation was greater than the counterclockwise rotation. They suggested that wave surge forces from the surface vessel and passive eccentric rotation of the foils were factors that affect the propulsive efficiency of the wave glider. Followed the study of Yang et al. [105], Yang et al. [49] further focused on the six tandem foils with passive pitch and conduced parametric studies. The results reported that for a 2D single foil the best pivot axis on it was the leading edge and for the six foils, the optimum torsional spring stiffness k_p was 0.8 N m/rad (frequency ratio = 25) in 2D simulation and 11.8 N m/rad (frequency ratio = 17) in 3D. Qi et al. [101] studied the mass ratio effect – density ratio of the foil to water – of a 2D flapping foil on wave glider with FVM. The foil was semi-active with a full-prescribed harmonic heaving motion and a passive pitching motion. With the increase in the mass ratio, the mean output power of the flapping foil decreases monotonously at high reduced frequency k and increases at low k,

Table 1
The CFD studies of WDP.

Investigators	Foil related information					Numerical methodology								Method
Reference	Foil shape	Regular waves and irregular waves	Motion	Environment	Application	2D/3D	CFD type	Method	Solving equation	Turbulence model	Regular waves and irregular waves	Grid	Mesh technology	
[90]	NACA0012	Rigid	Active	Regular waves and irregular waves	Ship propulsion	3D	Regular waves and irregular waves	FVM	RANSE	SST k-ω	VOF	Unstructured grid	–	FVM
[91]	NACA0008	Rigid	Semi-active	Regular waves	Physical mechanisms	2D	FLUENT	FEM	RANS	RNG k-ϵ	No free surface	Unstructured grid	–	FEM
[92]	NACA0008	Rigid	Regular waves and irregular waves	Regular waves	Wave-powered vehicle	2D	FLUENT	–	RANS	RNG k-ϵ	No free surface	Unstructured grid	Dynamic mesh	-
[52]	NACA0012	Rigid	Semi-active	No wave	Wave glider	2D	Regular waves and irregular waves	–	URANS	SST k-ω	No free surface	Structured grid	Overset mesh	-
[31]	NACA0008	Rigid	Semi-active	Uniform flow	Wave glider	2D	FLUENT	–	RANS	RNG k-ϵ	No free surface	Unstructured grid	Dynamic mesh	-
[93]	Regular waves and irregular waves	Rigid	Active	Uniform flow	Wave glider	3D	STAR-CCM+	–	RANS	k-ω	No free surface	Structured grid	Overset mesh	-
[94]	NACA0012	Rigid	Regular waves and irregular waves	Regular waves and irregular waves	Ship propulsion	3D	In-house CFD	FVM	URANS	–	VOF	Structured grid	–	FVM
[95]	NACA0012	Rigid	Semi-active	Regular waves	Wave glider	2D	Regular waves and irregular waves	–	RANS	SST k-ω	No free surface	Unstructured grid	Dynamic mesh	-
[96]	NACA0012	Rigid	Passive	Regular waves	Wave glider	2D	FLUENT	–	RANS	k-ϵ	No free surface	Unstructured grid	Dynamic mesh	-
[97]	NACA0015	Rigid	Semi-active	Regular waves	Wave glider	2D	FLUENT	FVM	URANS	SST k-ω	No free surface	Structured grid	Overset mesh	FVM
[98]	NACA0012	Rigid	Semi-active	Regular waves	Wave glider	2D	Custom C++	FDM	LES	–	No free surface	Cartesian grid	–	FDM
[53]	NACA0015	Rigid	Passive	Regular waves	Physical mechanisms	2D	In-house CFD	FVM	RANS	–	LSM	Cartesian grid	–	FVM
[51]	NACA0012	Rigid	Semi-active	No wave	Wave glider	2D	FLUENT	FVM	URANS	SST k-ω	No free surface	Structured grid	Overset mesh	FVM
[99]	–	Rigid	Passive	Regular waves	Regular waves and irregular waves	3D	Regular waves and irregular waves	–	–	–	VOF	Unstructured grid	–	-
[26]	NACA0015	Rigid	Passive	Irregular waves	Regular waves and irregular waves	3D	Regular waves and irregular waves	–	RANS	RNG k-ϵ	VOF	Structured grid	Overset mesh	-
[36]	NACA0012	Rigid	Active	No wave	Physical mechanisms	2D	FLUENT	FVM	RANS	S-A	No free surface	Regular waves and irregular waves	–	FVM
[100]	NACA0012	Rigid	Passive	Regular waves	Wave-driven catamaran	3D	STAR-CCM+	–	RANS	RNG k-ϵ	VOF	Structured grid	Overset mesh	-
[45]	NACA0015	Rigid	Active	Regular waves	Ship propulsion	2D	FLUENT	–	RANS	SST k-ω	–	Structured grid	Overset mesh	-
[101]	NACA0012	Rigid	Semi-active	No wave	Wave glider	2D	FLUENT	FVM	URANS	S-A	No free surface	Regular waves and irregular waves	–	FVM
[102]	NACA0008	Rigid	Semi-active	No wave	Wave glider	2D	FLUENT	FEM	Regular waves and irregular waves	–	No free surface	Unstructured grids	Dynamic mesh	FEM
[39]	NACA0012	Rigid	Active	Regular waves	AUV	3D	Star CCM+	–	RANS	k-ϵ	No free surface	Structured grid	Overset	-
[103]	Regular waves and irregular waves	Rigid	Active	Regular waves and irregular waves	Regular waves and irregular waves	2D	Regular waves and irregular waves	FVM	RANS	SST k-ω	VOF	Regular waves and irregular waves	–	FVM
[37]	NACA0012	Rigid	Active	No wave	Regular waves and irregular waves	2D	FLUENT	FVM	URANS	S-A	No free surface	Unstructured grid	Dynamic mesh	FVM
[104]	–	Rigid	Active	Regular waves	Regular waves and irregular waves	3D	Regular waves and irregular waves	FVM	–	SST k-ω	VOF	Unstructured grid	Dynamic mesh	FVM
[49]	NACA0012	Rigid	Semi-active	Uniform flow	Wave glider	2D,3D	STAR-CCM+	–	Regular waves and irregular waves	–	No free surface	Structured grid	Overset mesh	-
[70]	NACA0012	Flexible	Active	Regular waves	Regular waves and irregular waves	2D	FLUENT	–	RANS	RNG k-ϵ	VOF	Unstructured grid	Dynamic mesh	-
[105]	NACA0012	Rigid	Semi-active	Regular waves	Wave glider	3D	Regular waves and irregular waves	FVM	URANS	SST k-ω	VOF	Unstructured grid	Regular waves and irregular waves	FVM
[106]	NACA0018	Rigid	Active	Regular waves	Ship propulsion	2D	Regular waves and irregular waves	–	RANS	SST k-ω	VOF	Unstructured grid	Dynamic mesh	-
[107]	NACA0012	Rigid	Active	Regular waves	Wave glider	2D	FLUENT	Regular waves and irregular waves	RANS	RNG k-ϵ	No free surface	Unstructured grid	Dynamic mesh	FVM
[108]	NACA0015	Rigid	Active	Uniform flow	WDPS concept	2D	–	–	RANS	RNG k-ϵ	No free surface	–	–	-
[109]	Flat plate	Rigid	Active	Uniform flow	Underwater vehicles	2D	–	FDM	–	–	–	Boundary-fitted grid	–	FDM
[110]	NACA0012	Rigid	Active	No wave	Ship propulsion	2D	FLUENT	–	RANS	k-ϵ	No free surface	Unstructured grid	Dynamic mesh	-
[34]	NACA0015	Rigid	Active	Regular waves	Physical mechanisms	2D	FLUENT	Regular waves and irregular waves	RANS	SST k-ω	VOF	Unstructured grid	Dynamic mesh	FVM

whereas as the mass ratio increases in the case of critical k, the average output power coefficient increases and decreases. Feng et al. [31] compared the characteristics of linear (torsion) and nonlinear (tension) springs mounted on the foils of wave glider. Fig. 21 illustrated that, for the same wave condition, the forward speed and propulsion force of a propulsion mechanism with a non-linear spring is greater than that of a linear spring. Sang et al. [95]'s numerical model simulated the float response of another USV type (named single-body architecture wave glider (SAWG), see Fig. 22) by AQWA and the derived motion of semi-active flapping foils attached to the USV by Fluent without wave surface. They presented the average forward velocity under different spring constants and wave frequencies (Fig. 23). After the verification of the model by tank experiment and sea trial, they suggested there is an optimum spring constant at different wave frequencies for maximum forward velocity, for example an optimum spring constant of 6 N m/rad at a wave frequency of 0.4 Hz Qingdao offshore. Wang et al. [98] proposed a mechanism that allowed the foil in the wave glider to harvest energy while propulsion and simulated the energy harvesting performances by a custom C++ procedure using immersed boundary and large eddy simulation methods. The harvested energy was used to provide the energy required to actuate the pitch of the semi-active foil. When the wave glider was traveling upstream, the oscillating foil can only function as a propeller; when the wave glider was traveling downstream, the oscillating foil can act as a propeller and an energy generator. Sang et al. [96] presented a self-adjusting lower limit (SALL) mechanism for wave glider optimization. This mechanism can passive control the maximum swing angle of foil in a counterclockwise direction according to the umbilical cable inclination angle. The CFD simulation results showed that the thrust of the SALL underwater glider increased by 17.78%, 7.42% and 20.70% compared to a conventional underwater glider when the stiffness coefficient of the torsion spring was k_p = 4 N m/rad, k_p = 6 N m/rad and k_p = 8 N m/rad respectively. While wave gliders continue to be the primary focus of research, it is worth noting that foils are also being explored for their application in other types of ASVs. Ci et al. [39] discussed about the structural optimization of the foil applied on the autonomous underwater vehicles (AUV), such as REMUS 100 AUV, using 3D CFD approaches—Star CCM+ and suggested that trapezoid foil with the NACA0012 section, i.e. the ratio of LE to TE of the foil = 1:2, had better performance. Liu et al. [70] studied the performance of a 2D flexible flapping foil in regular waves for unmanned underwater vehicles propulsion. The method was validated by rigid foil experiments and further analysis also compared with rigid foil under the same flow conditions. In the case of larger wave amplitudes or smaller wavelengths, both fixed and

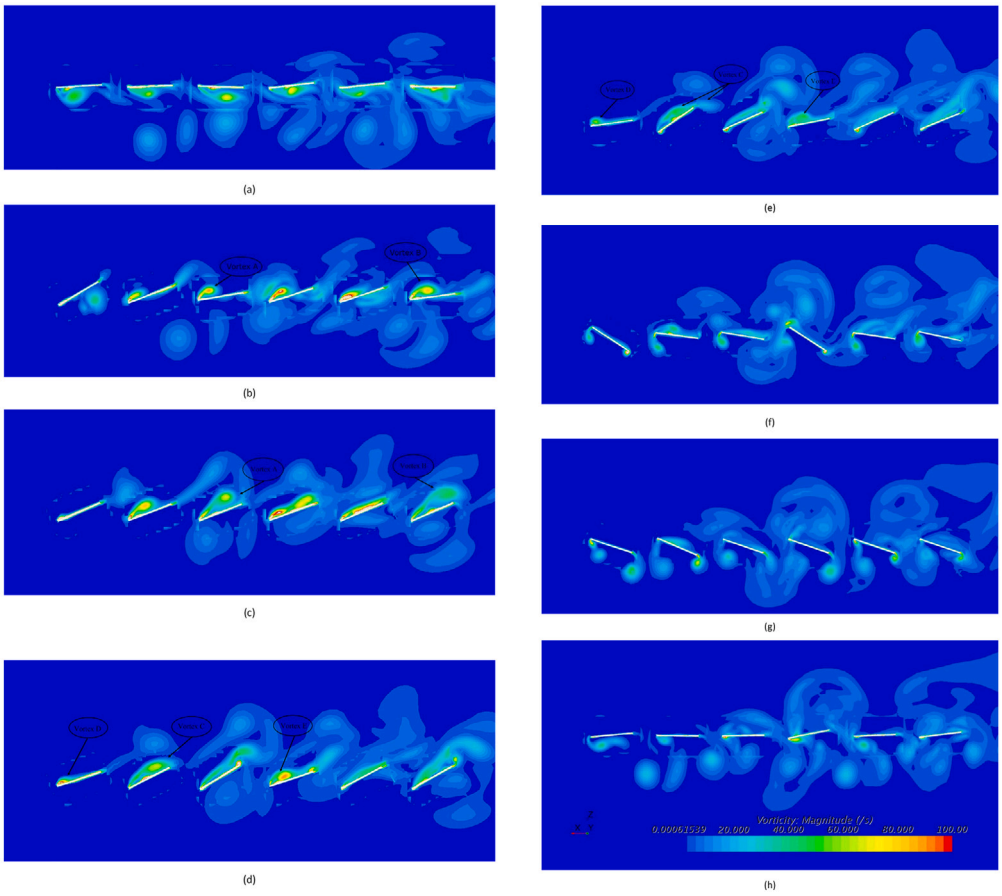

Fig. 20. Time series of the vorticity magnitude development in one cycle of the foil (a) $t = 0$, (b) $t = 0.175$, (c) $t = 0.3$, (d) $t = 0.4$, (e) $t = 0.5$, (f) $t = 0.66$, (g) $t = 0.8$, (h) $t = 1.0$. (Yang et al. [105]).

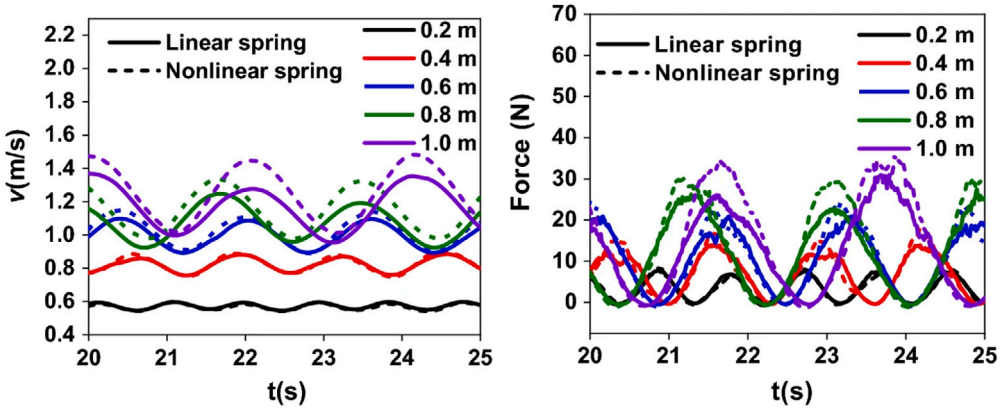

Fig. 21. Forward velocity and propulsion force (right) under different sea conditions. (Feng et al. [31]).

flexible foils are able to generate higher thrusts, see Fig. 24. The flexible deformation of the foil not only helps to increase the vortex strength, but also reduces the dissipation of vortex energy in the flow field. Higher performance is achieved when the foil moves at a frequency equal to that of the wave it encounters. The phenomenon has likewise been observed by Xu et al. [86] in their study of active rigid foil in nonlinear waves.

Furthermore, researchers have also directed their attention towards investigating the utilization of foils in ship propulsion, expanding the scope of foil applications beyond ASVs. Zhang et al. [26] proposed a novel type of the retractable wave foil. 4 pairs tandem foils placed on both sides of the ship (Fig. 25). The foils can be unfold in rough seas and passively change the angle of attack. The CFD result by STAR-CCM + were validated by mathematical simulation in Simulink. Fig. 26 showed the ship propulsion and anti-pitching moments generated by the foil for different wave encounter angles. It was noticed that when the wave encounter angle is 180°, the thrust and moment of the ship was the largest. Therefore, the wave excitation to the ship is the maximum in the head wave, which was also confirmed by Li et al. [111] with the study of Natural-energy-driven surface vehicle (NSV). Zhang et al. [99] introduced a novel way for the foil to be equipped to the hydraulic device, the pitch of the wave foil was passively adjusted by spring damping and the wave foil can be retracted and expanded by a strut connected to the hull. The time-domain simulations and wave-ship-foil

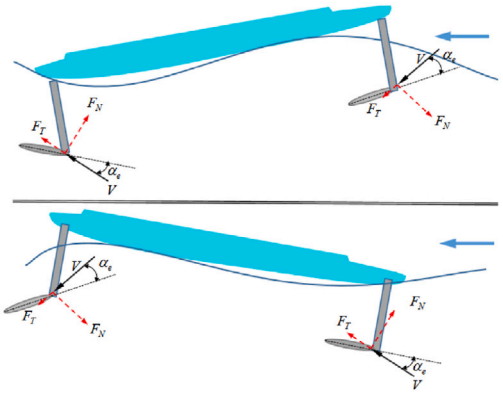

Fig. 22. The wave propulsion principle of the SAWG. (Sang et al. [95]).

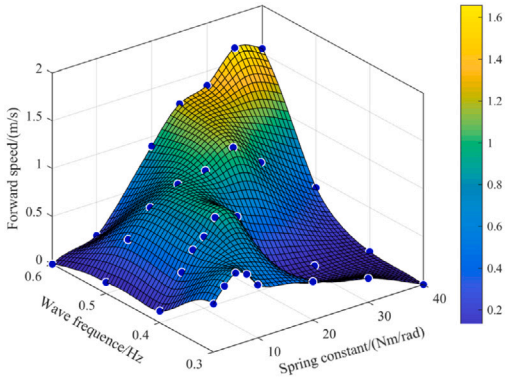

Fig. 23. The mean forward speed responses for varied spring constants and wave frequencies. (Sang et al. [95]).

coupling simulations were conducted by Simulink and STAR-CCM+. The CFD results showed that passive pitching adjustment facilitates better extraction of wave energy and anti-pitching performance. By retracting the foils when not in use, ships can reduce drag and increase fuel efficiency. However, in the case of conventional foil designs that are attached and non-retractable, different considerations come into play. Moreira et al. [45] presented a 2D parametric study of dual flapping foils system. They focused on evaluating the ship propulsion and energy harvesting performance of foils and placed the dual foils in various unaligned or out-of-phase positions. Under the same sea state, higher obtained energy and hydrodynamic coefficients (C_t, C_l and C_P) were obtained for foils with larger horizontal spacing (cases 1-2) compared to those with smaller horizontal spacing (cases 3-4). Similar to Mermaid II, the catamaran type ship brings to attention for wave propulsion. Wang et al. [104] analyzed 3D low-speed wave-powered unmanned catamaran ship (Fig. 27) motion without/with horizontally fixed foils under head wave through both potential theory (AQWA) and the CFD method (Fluent). The results showed horizontal forces acting on the tandem foils provided thrust to propel the ship while vertical force on the catamaran with foils was smaller than that of without foils therefore decreased the heave and pitch motions of the ship and the wave-added resistance on the ship. Zhang et al. [100] simulated the same type of catamaran by the combination of multi-body dynamics model and STAR-CCM+. Just as the bowfoil worked better than stern-foil, the foil thrust was found to be much greater at the bow of the catamaran than at the stern, as the front foil heaved more than the aft foil. They also concluded that the motion of the catamaran completely driven by wave and its advancing speed was positively correlated with wave height and negatively correlated with wavelength. In the context of numerical simulation of bow foil, an innovative project on ship dual-fuel engines and propulsion is proposed, called the SeaTech Horizon 2020 project, H2020 project for short [112]. Fig. 28 illustrated the model of bow foil in H2020 project. This project provide a renewable-energy-based hybrid solution for the reduction of fuel consumption and operational cost. Belibassakis et al. had presented a preliminary analysis of the proposed bow foil and ship engines in waves as part of this project [113–115] using lab test and BEM and CFD simulation. In the study, the additional thrust generated by the foil allowed the engine to run at partial load without affecting the speed of the ship and resulting less CO2 emissions. Ntouras et al. [94] also confirmed the feasibility of a static foil bow with a non-zero AoA as a trim-pitch stabilizer in head waves by experimental data in towing tank and in-house CFD simulation result. Both numerical and experimental results showed the significant decrease in added resistance in the waves of the 12%–34% compared to the bare hull. Furthermore, the economics of bow foil thrusters were studied by Ventikos et al. [116]. Their proposed Life Cycle Cost Analysis (LCCA) framework includes construction, operation, maintenance and end-of-life. The operating cost model result proved that the foil thruster proposed by H2020 Project is economically promising through the expected engine power demands.

Moreover, the research endeavors extend to exploring the implementation of foils in other innovative marine systems, showcasing the diverse range of applications for foils beyond ASV and ship propulsion. Kumar and Shin [124,125] conducted a series of experiments to explore the practical application of foils in designing station-keeping systems for deep-water floaters. They [124,125] investigated and measured the thrust force generated by a rigid foil attached to an elastic plate, which underwent flapping motion in a wave flume. Their empirical studies led to the development of an empirical formula that incorporates azimuth angles, allowing for the prediction of thrust force for a flapping foil. This formula was derived through multiple regression analysis of their experimental data. Additionally, Kumar and Shin [103] extended their predictions by employing CFD method. Utilizing a Two-way Fluid—Structure Interaction (FSI) method, they examined the interaction between a submerged actively flapping foil and the surrounding fluid in short waves. The geometry in [103] was the same as in experiments, see Fig. 29. The thrust forces were evaluated at five different flapping frequencies and the results showed that the positive force from the active foil were dominating and then can benefit the design of a station-keeping system of a floater in short waves while passive foil proved ineffective in the experiment [124].

5.3. Brief discussion of numerical result

In the reported numerical study of wave-induced propulsion, the influence of the flapping foil was detailed and various parameters were studied. Both potential flow solver and Navier–Stokes flow solver were used. The submergence depth was found to be a significant factor, with shallower depths generally converting more wave energy and generating more thrust, but wave resistance becoming a significant issue in some cases. The presence of the free surface was also found to be important, but its effect became less significant with increasing heave amplitude and pitch angle. Finally, the results showed that head waves performed better for wave excitation propulsion and generated more anti-pitching moments to boost ship stability.

6. WDP applications (WDPS)

This chapter aims to provide an overview of the various industrial applications of wave propulsion technology, specifically those that have reached full scale size and have been proven in practice. The focus will be on the use of WDP in unmanned surface vehicles, the shipping industry, and other industries such as the offshore industry. The knowledge gained from the theoretical, experimental, and numerical studies discussed in previous chapters will be applied to these real-world scenarios to demonstrate the potential of wave propulsion technology.

Table 2
The applications of WDPS on manned vessels.

Year	Creator	Location	Ship	Ref.
1895	Herman Linden	Naples, Italy	'Autonaut'	[73]
1935	Unkown	Long Beach, Califonia, USA	18-inch model	[117]
1950	John S. McCubbin	Victoria, Australia	–	[118]
1966	Joseph A. Gause	Burlington, Ontario, Canada	Gausefin I	[119]
1981	Einar Jacobsen	–	Kystfangst	[120,121]
2008	Yukata Terao	Tokai University, Japan	Suntory Mermaid II	[80]
2012	MARIN	Netherlands	O-foil	[122]
2013	Rolls-Royce, MOST and SeaSpeed	UK	Wave Augmented Foil Technology (WAFT)	[25]
2014	Dolprop	Ekerö, Sweden	Fluke	[123]
2019	WAVEFOIL	Norway	SmartWings	[17]

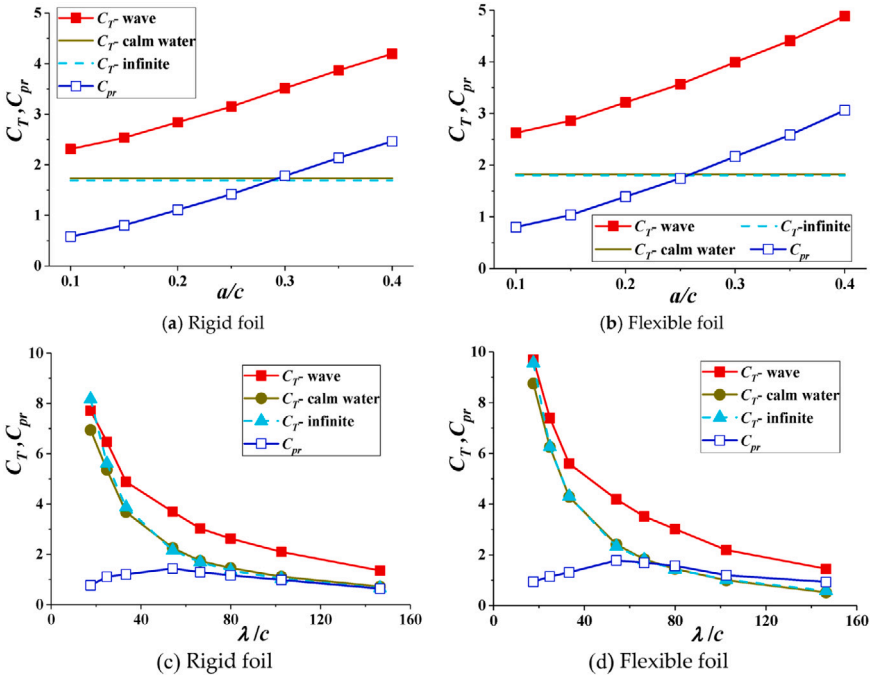

Fig. 24. (a) (b) Average thrust and wave power utilization coefficients for the foil versus non-dimensional wave amplitudes. (c) (d) The average thrust and wave power utilization coefficients for the foil versus non-dimensional wavelengths. (Liu et al. [70]).

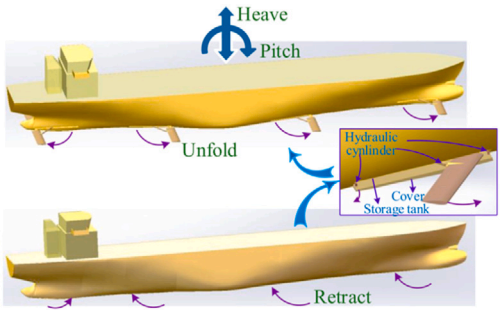

Fig. 25. The ship with retractable flapping foils. (Zhang et al. [26]).

6.1. Foil with manned vessels

A full list of applications for foil-attached manned vessels is provided in Table 2. The idea of using wave-powered foils for marine propulsion dates back to 1895, when Linden proposed a British patent for a ship equipped with a flexible foil at the bow [73]. One of the most notable examples of this technology in practice is the Suntory Mermaid II [80], a wave-powered boat that successfully completed a 110-day voyage from Honolulu, Hawaii to the Kii Channel, Japan under the leadership of Captain Kenichi Horie. This journey demonstrated the potential of foil propulsion for eco-sailing and gained international attention. More recently, the WAVEFOIL company has developed technology for retractable bow foils attached to ships [126] and has expanded its applications from 2019 onwards. These foils are used on a wide range of vessels, from large 45 meter passenger ships to small 23 meter ambulance vessels.

6.2. Foil with unmanned surface vehicles (USV)

Foil-attached unmanned vessels have been gaining increasing attention as a promising solution for oceanic applications, e.g. monitoring. These vessels utilize the energy from ocean waves to provide propulsion, enabling them to perform long-duration missions with limited energy consumption. A comprehensive list of these applications can be found in Table 3.

There are two primary mechanisms for underwater foil wave propulsion: heave-induced gliding and pitch-induced flapping [127]. The heave-induced mechanism uses the motion of the vessel to generate a flow over submerged foils, similar to an aerial glider with umbilical

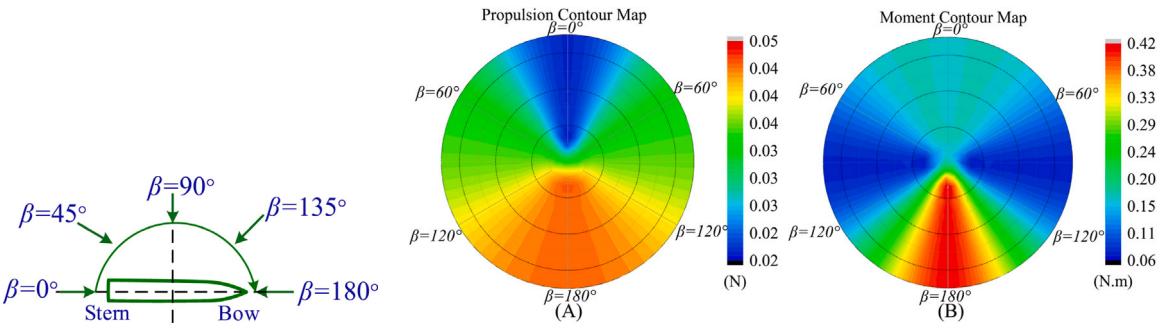

Fig. 26. The contour map for the propulsion (A) and moment (B) with different encounter angle. (Zhang et al. [26]).

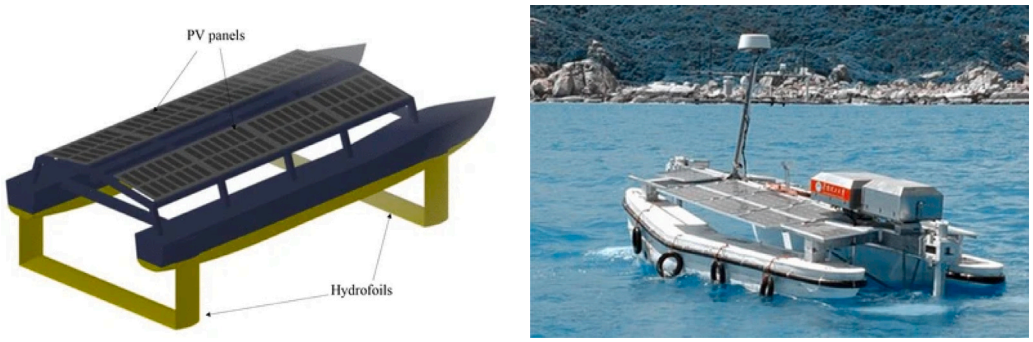

Fig. 27. The unmanned catamaran ship completed driven by foils (Wang et al. [104]).

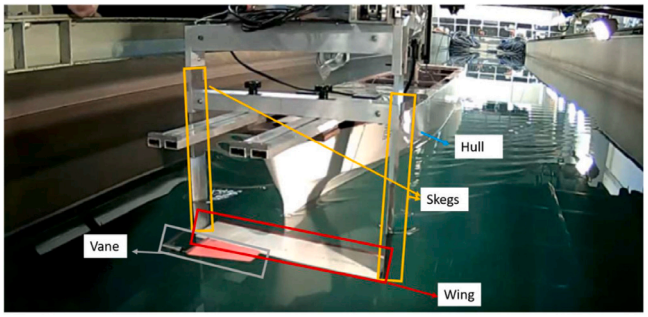

Fig. 28. SeaTech Horizon 2020 project: Experimental configuration of the dynamic wing arranged at the bow of the ferry ship model tested. (Ntouras et al. [94]).

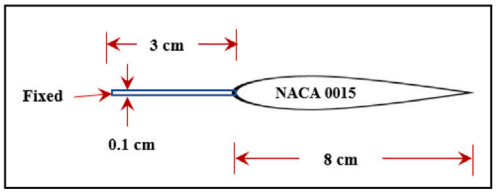

Fig. 29. The flapping foil with an elastic plate attached to the leading edge. (Kumar and Shin [103,124]).

cables. The pitch-induced mechanism utilizes the movement of the vessel to drive the foil in a flapping motion, interacting with the incoming wave's oscillating flow to produce thrust. Commercial USVs, such as the Liquid Robotics' Wave Glider and AutoNaut's AutoNaut, have utilized both of these propulsion methods [14,15]. A wave glider typically consists of a floating body, an underwater propulsion mechanism, and a connecting cable between the two, as shown in Fig. 30(a). The floating body captures wave energy, converting it into heave motion to drive the underwater propulsion mechanism through the connecting structure. Placing the glider in a deeper position helps to avoid surface wave turbulence and maintain stability. An AutoNaut, on the other hand, is an USV with submerged flapping foils fixed to the hull both at the bow and stern via a rigid arm, as shown in Fig. 30(b). The motion of the vessel caused by waves drives the spring-loaded submerged foils, forcing them to flap at the frequency of the incoming waves. In recent years, multi-energy source NSVs have also been proposed, as demonstrated by Li et al. [111]. These vessels can be powered by multiple natural energy sources, including wave, wind, and solar energy, as illustrated in Fig. 31. When sailing at its design speed of 1.5 m/s, it is capable of absorbing natural energy to replenish its own energy consumption.

Table 3
The applications of WDPS on unmanned vessels.

Year	Creator	Location	USV	Ref.
2007	Liquid Robotics	USA	Wave Glider	[14]
2013	AutoNaut	UK	AutoNaut series	[16]
2014	Team of Ocean Mobile Observation Technology (TOMOT)	China	Black Pearl	[128]
2021	Li Ye et al.	China	NSV	[111]
2022	Hongqiang Sang et al.	China	SAWG	[95]

6.3. Foil with other structures

The utilization of foils for wave propulsion is not limited to marine vessels alone. Another application of this technology is the wave energy converters (WECs). One such example is the wave-bladed cyclorotors, which uses foils to generate lift force by the wave-induced water

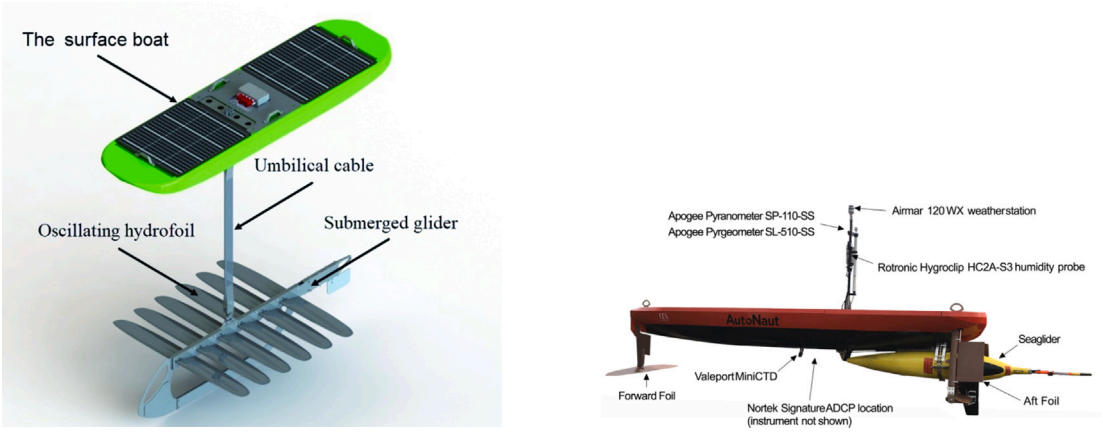

(a) Wave Glider (Qi et al. [37]) (b) Caravela (an AutoNaut vessel) (Siddle et al. [128])

Fig. 30. The commercial USVs from Liquid Robotics and AutoNaut [129].

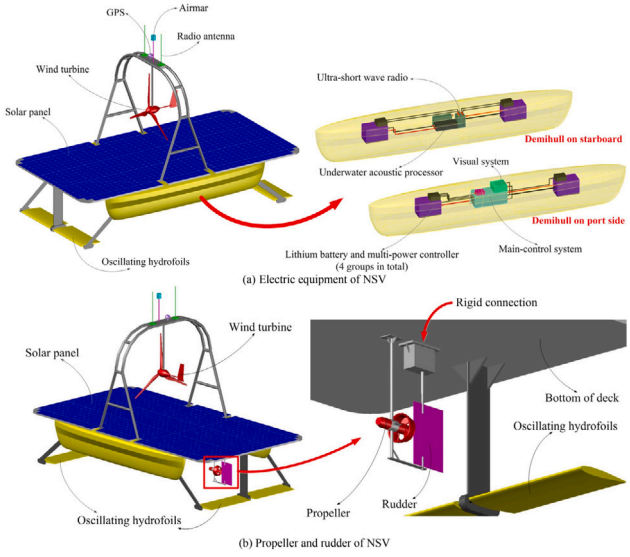

Fig. 31. Basic structure and electric equipment of NSV. (Li et al. [111]).

velocities, and then rotates around an axis continuously. For instance, the LiftWEC concept, which uses two foils to spin, has been proposed as a novel WEC [130]. Further information on cycloidal WECs can be found in works such as [130,131].

Offshore platforms, including both offshore wind and offshore Photovoltaics (PV) platforms, operate in wave conditions and are subject to wave loads and wave-induced motions. These motions are undesirable as they increase maintenance and mooring costs. While WDPS has the potential to propel or stabilize floating systems using flapping foils, there have been no documented examples of WDPS being applied to offshore platforms. The authors believe that this is an area with significant potential and is in need of further research and development.

7. Conclusion

WDP has the potential to be highly efficient and environmentally friendly propulsion, but more research and development is needed to overcome the challenges and limitations. Future research directions include exploring the generation of the reversed von Kármán vortex street, understanding the foil-ship hull-wave interaction, the optimal number and placement of foils on ships, optimizing the ship size, foil size, and submergence depth, analyzing the economic aspects of WDP, optimizing the 3D foil design, developing an efficient control mechanism, examining the effect of spring and wave conditions on passive foils, the investigation of foil flexibility effects on the performance enhancement and stability of the system and further developing applications in the offshore industry.

Declaration of competing interest

The authors declare that they have no known competing financial interests or personal relationships that could have appeared to influence the work reported in this paper.

Data availability

No data was used for the research described in the article.

Acknowledgments

J. Xing acknowledges the support by the China Scholarship Council (CSC) from the Ministry of Education of P.R. China. Dr. L. Yang acknowledge the support from the Department for Transport's (DfT) Transport Research and Innovation Grants (TRIG): G-TRANSPORT: greening transportation of cargo ships via hybrid wave propulsion and British Council: Feasibility study of hybrid propulsion for unmanned surface vehicle for environmental monitoring.

References

[1] Knoller R. Die gesetzedes luftwiderstandes. Flug-und Mot (Wien) 1909;3(21):1–7.
[2] Betz A. Ein beitrag zur erklaerung segelfluges. Z Flugtech Mot 1912;3:269–72.
[3] Katzmayr R. Effect of periodic changes of angle of attack on behavior of airfoils. Tech. rep., 1922.
[4] McKinney W, DeLaurier J. Wingmill: an oscillating-wing windmill. J Energy 1981;5(2):109–15.
[5] Lighthill SJ. Mathematical biofluiddynamics. SIAM; 1975.
[6] von Karman T. General aerodynamic theory-perfect fluids. Aerodyn Theory 1935;2:346–9.
[7] Koochesfahani MM. Vortical patterns in the wake of an oscillating airfoil. AIAA J 1989;27(9):1200–5.
[8] Jones K, Dohring C, Platzer M. Wake structures behind plunging airfoils-a comparison of numerical and experimental results. In: 34th Aerospace sciences meeting and exhibit. 1996, p. 78.
[9] Buchholz JH, Smits AJ. The wake structure and thrust performance of a rigid low-aspect-ratio pitching panel. J Fluid Mech 2008;603:331–65.
[10] Godoy-Diana R, Marais C, Aider J-L, Wesfreid JE. A model for the symmetry breaking of the reverse bénard–von kármán vortex street produced by a flapping foil. J Fluid Mech 2009;622:23–32.
[11] Lagopoulos N, Weymouth G, Ganapathisubramani B. Universal scaling law for drag-to-thrust wake transition in flapping foils. J Fluid Mech 2019;872.

[12] Jakobsen E, et al. The foilpropeller, wave power for propulsion. 1981.
[13] Terao Y. A floating structure which moves toward the waves (possibility of wave devouring propulsion. 1982.
[14] Hine R, Willcox S, Hine G, Richardson T. The wave glider: A wave-powered autonomous marine vehicle. In: OCEANS 2009. IEEE; 2009, p. 1–6.
[15] Johnston P, Poole M. Marine surveillance capabilities of the AutoNaut wave-propelled unmanned surface vessel (USV). In: OCEANS 2017-Aberdeen. IEEE; 2017, p. 1–46.
[16] AutonautusV. 2023, URL https://autonautusv.com/vessels-0. (Accessed on 17 June 2023).
[17] Yrke A, Bøckmann E. Full-scale experience with retractable bow foils on m/f teistin. 2019, URL https://wavefoil.com/wp-content/uploads/2019/12/Full-scale-experience-with-retractable-bow-foils-on-MF-Teistin.pdf. (Accessed on 17 June 2023).
[18] Lidtke AK, Humphrey VF, Turnock SR. Feasibility study into a computational approach for marine propeller noise and cavitation modelling. Ocean Eng 2016;120:152–9.
[19] Kimmerl J, Mertes P, Abdel-Maksoud M. Turbulence modelling capabilities of iles for propeller induced urn prediction. In: SNAME maritime convention. OnePetro; 2020.
[20] Malefaki I, Belibassakis K. A novel FDTD–PML scheme for noise propagation generated by biomimetic flapping thrusters in the ocean environment. J Marine Sci Eng 2022;10(9):1240.
[21] Malefaki I, Karperaki A, Belibassakis K. Noise generation and propagation from flapping-foil thrusters used for marine propulsion. In: International conference on offshore mechanics and arctic engineering, vol. 85901. American Society of Mechanical Engineers; 2022, V05BT06A053.
[22] Belibassakis K, Prospathopoulos J, Malefaki I. Scattering and directionality effects of noise generation from flapping thrusters used for propulsion of small ocean vehicles. J Marine Sci Eng 2022;10(8):1129.
[23] Wu X, Zhang X, Tian X, Li X, Lu W. A review on fluid dynamics of flapping foils. Ocean Eng 2020;195:106712.
[24] Bøckmann E, Steen S. Experiments with actively pitch-controlled and spring-loaded oscillating foils. Appl Ocean Res 2014;48:227–35.
[25] Bøckmann E, Steen S. Model test and simulation of a ship with wavefoils. Appl Ocean Res 2016;57:8–18.
[26] Zhang Y, Xu L, Ding Z, Hu M. Wave propulsion and sea-keeping enhancement for ships in rough sea condition by flapping foils. Ocean Eng 2022;266:112802.
[27] Yoshida H, Yamasaki K, Sunahara S. Application of wave devouring propulsion technology to support positioning of floating structure. In: International conference on offshore mechanics and arctic engineering, vol. 51203. American Society of Mechanical Engineers; 2018, V001T01A024.
[28] Anevlavi DE, Filippas ES, Karperaki AE, Belibassakis KA. A non-linear BEM–FEM coupled scheme for the performance of flexible flapping-foil thrusters. J Marine Sci Eng 2020;8(1):56.
[29] Fernandez-Prats R. Effect of chordwise flexibility on pitching foil propulsion in a uniform current. Ocean Eng 2017;145:24–33.
[30] Zhu Q. Numerical simulation of a flapping foil with chordwise or spanwise flexibility. AIAA J 2007;45(10):2448–57.
[31] Feng Z, Chang Z, Deng C, Zhao L, Chen J, Zhang J, et al. Effects of nonlinearity of restoring springs on propulsion performance of wave glider. Nonlinear Dynam 2022;108(3):2007–22.
[32] Platzer MF, Jones KD, Young J, Lai JC. Flapping wing aerodynamics: progress and challenges. AIAA J 2008;46(9):2136–49.
[33] Pedro G, Suleman A, Djilali N. A numerical study of the propulsive efficiency of a flapping hydrofoil. Int J Numer Methods Fluids 2003;42(5):493–526.
[34] De Silva LWA, Yamaguchi H. Numerical study on active wave devouring propulsion. J Marine Sci Technol 2012;17(3):261–75.
[35] Meng J, Cao Y, Chao L, Li L. Study on efficiency of flapping foil propulsion with different motion patterns. In: OCEANS 2017-Aberdeen. IEEE; 2017, p. 1–5.
[36] Gao P, Huang Q, Pan G. Propulsion performance and wake dynamics of heaving foils under different waveform input perturbations. J Marine Sci Eng 2021;9(11):1271.
[37] Qi Z, Zhai J, Li G, Peng J. Effects of non-sinusoidal pitching motion on the propulsion performance of an oscillating foil. PLoS One 2019;14(7):e0218832.
[38] Read DA, Hover F, Triantafyllou M. Forces on oscillating foils for propulsion and maneuvering. J Fluids Struct 2003;17(1):163–83.
[39] Ci X, Fan S, Jin Y. Design and operation optimization of the flapping fin for auv propulsion. In: 2019 IEEE underwater technology. IEEE; 2019, p. 1–9.
[40] Streitlien K, Triantafyllou G. On thrust estimates for flapping foils. J fluids Struct 1998;12(1):47–55.
[41] Ramamurti R, Sandberg W. Computational study of 3-D flapping foil flows. In: 39th Aerospace sciences meeting and exhibit. 2001, p. 605.
[42] Bohl DG, Koochesfahani MM. MTV measurements of the vortical field in the wake of an airfoil oscillating at high reduced frequency. J Fluid Mech 2009;620:63–88.
[43] Terao Y, Sakagami N. Application of wave devouring propulsion system for ocean engineering. In: International conference on offshore mechanics and arctic engineering. 55393, American Society of Mechanical Engineers; 2013, V005T06A051.
[44] Terao Y, Sakagami N. Design and development of an autonomous wave-powered boat with a wave devouring propulsion system. Adv Robot 2015;29(1):89–102.
[45] Moreira D, Mathias N, Morais T. Dual flapping foil system for propulsion and harnessing wave energy: A 2D parametric study for unaligned foil configurations. Ocean Eng 2020;215:107875.
[46] Triantafyllou M, Triantafyllou G, Gopalkrishnan R. Wake mechanics for thrust generation in oscillating foils. Phys Fluids A Fluid Dyn 1991;3(12):2835–7.
[47] Cleaver DJ, Wang Z, Gursul I. Bifurcating flows of plunging aerofoils at high strouhal numbers. J Fluid Mech 2012;708:349–76.
[48] Zurman-Nasution A, Ganapathisubramani B, Weymouth G. Influence of three-dimensionality on propulsive flapping. J Fluid Mech 2020;886.
[49] Yang F, Shi W, Wang D. Systematic study on propulsive performance of tandem hydrofoils for a wave glider. Ocean Eng 2019;179:361–70.
[50] Thaweewat N, Phoemsapthawee S, Juntasaro V. Semi-active flapping foil for marine propulsion. Ocean Eng 2018;147:556–64.
[51] Zhang Y, Feng Y, Chen W, Gao F. Effect of pivot location on the semi-active flapping hydrofoil propulsion for wave glider from wave energy extraction. Energy 2022;255:124491.
[52] Chen W, Zhang Y, Gao F. Experimental and numerical studies on the torsion stiffness effect of a semi-active flapping hydrofoil propulsion. Ocean Eng 2022;265:112578.
[53] Xing J, Stagonas D, Hart P, Zhang C, Yang J, Yang L. Wave induced thrust on a submerged hydrofoil: pitch stiffness effects. 2022, arXiv preprint arXiv:2209.05551.
[54] Weinblum GP. Approximate theory of heaving and pitching of hydrofoils in regular shallow waves. David W Taylor model basin, navy department, report C-479, hydromechanics laboratory, research and development report, 1954.
[55] Wu T, et al. Extraction of flow energy by a wing oscillating in waves. J Ship Res 1972;16(01):66–78.
[56] Isshiki H. A theory of wave devouring propulsion (1st report) thrust generation by a linear wells turbine. J Soc Naval Archit Japan 1982;1982(151):54–64.
[57] Filippas E, Belibassakis K. Free surface effects on hydrodynamic analysis of flapping foil thruster in waves. In: International conference on offshore mechanics and arctic engineering, vol. 55393. American Society of Mechanical Engineers; 2013, V005T06A043.
[58] Grue J, Mo A, Palm E. Propulsion of a foil moving in water waves.. J Fluid Mech 1988;186:393–417.
[59] Filippas E, Belibassakis K. Hydrodynamic analysis of flapping-foil thrusters operating beneath the free surface and in waves. Eng Anal Bound Elem 2014;41:47–59.
[60] Filippas ES, Papadakis GP, Belibassakis KA. Free-surface effects on the performance of flapping-foil thruster for augmenting ship propulsion in waves. J Marine Sci Eng 2020;8(5):357.
[61] Isshiki H, Murakami M. Wave power utilisation into ship propulsion. In: 5th Int symp. & exibit on offshore mechanics and arctic eengineering (OMAE) held at Tokyo. 1986.
[62] Isshiki H. Utilization of wave energy to improve propulsive and seekeeping performances of a ship in rough weather. Asian J Eng Technol 2015;3(6).
[63] Isshiki H, Murakami M. A theory of wave devouring propulsion (3rd report) an experimental verification of thrust generation by a passive-type hydrofoil propulsor. J Soc Naval Archit Japan 1983;1983(154):118–28.
[64] Lopes D, Falcão de Campos J, Sarmento A. An analytical model study of a flapping hydrofoil for wave propulsion. In: International conference on offshore mechanics and arctic engineering, vol. 51326. American Society of Mechanical Engineers; 2018, V11AT12A013.
[65] Rozhdestvensky KV, Htet ZM. A mathematical model of a ship with wings propelled by waves. J Mar Sci Appl 2021;20(4):595–620.
[66] Bowker J, Townsend N. A probabilistic method to evaluate bow foils for realistic seas and shipping routes. Appl Ocean Res 2022;129:103374.
[67] Rozhdestvensky K. Study of underwater and wave gliders on the basis of simplified mathematical models. Appl Sci 2022;12(7):3465.
[68] Isshiki H, Murakami M. A theory of wave devouring propulsion (4th report) a comparison between theory and experiment in case of a passive-type hydrofoil propulsor. J Soc Naval Archit Japan 1984;1984(156):102–14.
[69] Hao H, Ma Q, Liao K, Zheng X. Experimental studies on hydrodynamics of a floater-adjusted wave propulsion device. In: The 27th international ocean and polar engineering conference. OnePetro; 2017.
[70] Liu P, Liu Y, Huang S, Zhao J, Su Y. Effects of regular waves on propulsion performance of flexible flapping foil. Appl Sci 2018;8(6):934.
[71] Wang J, Santhosh S, Colomés O, Capaldo M, Yang L. Experimental study of dynamic response of passive flapping hydrofoil in regular wave. Phys. Fluids 2023;35(7):077127.
[72] Jakobsen E. The wing propeller, wave power for propulsion. In: 2nd International symp. on wave & tidal energy. BHRA Fluid Engineering; 1981, p. 363–8.
[73] Isshiki H. Wave energy utilization into ship propulsion by fins attached to a ship. In: The fourth international offshore and polar engineering conference. OnePetro; 1994.

[74] Isshiki H, Naito S. An application of wave energy -thrust generated by a hydrofoil in waves-. In: "Current practices and new technology in ocean engineering" symp . asme's ocean engineering division held at new orleans. 1986.
[75] Isshiki H, Hatta K, Terao Y. Research and development of oscillating hydrofoil propulsion utilizing wave energy. Bulle Soc Naval Archit Japan 1988;1988(719):18–26.
[76] Bøckmann E, Steen S. The effect of a fixed foil on ship propulsion and motions. In: Proceedings of the third international symposium on marine propulsors smp, vol. 13. 2013, p. 553–61.
[77] Bowker J, Townsend N. Evaluation of bow foils on ship delivered power in waves using model tests. Appl Ocean Res 2022;123:103148.
[78] Feng P, Ma N, Gu X. A practical method for predicting the propulsive performance of energy efficient ship with wave devouring hydrofoils at actual seas. Proc Inst Mech Eng M 2014;228(4):348–61.
[79] Huang S-W, Wu T-L, Hsu Y-T, Guo J-H, Tsai J-F, Chiu F-C. Effective energy-saving device of eco-ship by using wave propulsion. In: 2016 Techno-ocean. IEEE; 2016, p. 566–70.
[80] Terao Y. Wave devouring propulsion system: From concept to trans-pacific voyage. In: International conference on offshore mechanics and arctic engineering, vol. 43444. 2009, p. 119–26.
[81] McGregor R, Thomson G. Sea trials of wave propulsion of a yacht using a flexible fin propeller. Renew Energy 1997;10(2–3):335–8.
[82] Bowker J, Townsend N, Tan M, Shenoi R. Experimental study of a wave energy scavenging system onboard autonomous surface vessels (ASVs). In: OCEANS 2015-Genova. IEEE; 2015, p. 1–9.
[83] Bowker JA, Tan M, Townsend NC. Forward speed prediction of a free-running wave-propelled boat. IEEE J Ocean Eng 2020;46(2):402–13.
[84] Terao Y, Sunahara S. Application of a wave devouring propulsion system to ocean engineering. In: International conference on offshore mechanics and arctic engineering, vol. 44946. American Society of Mechanical Engineers; 2012, p. 207–14.
[85] Filippas E, Belibassakis K. A nonlinear time-domain BEM for the performance of 3D flapping-wing thrusters in directional waves. Ocean Eng 2022;245:110157.
[86] Xu G, Duan W, Zhou B. Propulsion of an active flapping foil in heading waves of deep water. Eng Anal Bound Elem 2017;84:63–76.
[87] Filippas E, Belibassakis K. Hydrodynamic analysis of flapping-foil thruster operating in random waves. In: International conference on offshore mechanics and arctic engineering, vol. 45509. American Society of Mechanical Engineers; 2014, V08AT06A023.
[88] Belibassakis KA, Politis GK. Hydrodynamic performance of flapping wings for augmenting ship propulsion in waves. Ocean Eng 2013;72:227–40.
[89] Belibassakis K, Filippas E. Ship propulsion in waves by actively controlled flapping foils. Appl Ocean Res 2015;52:1–11.
[90] Belibassakis K, Filippas E, Papadakis G. Numerical and experimental investigation of the performance of dynamic wing for augmenting ship propulsion in head and quartering seas. J Marine Sci Eng 2022;10(1):24.
[91] Chang Z, Feng Z, Deng C, Zhao L, Zhang J, Zheng Z, et al. Analysis of propulsion performance of wave-propelled mechanism based on fluid-rigid body coupled model. Proc Inst Mech Eng M 2022;236(3):713–25.
[92] Chang Z, Deng C, Feng Z, Chen J, Zheng Z, Zhang Y. Performance analysis of wave-powered vehicle by active control of the hydrofoil. Ocean Eng 2022;255:111358.
[93] Mouliswar R, Chandrasekaran K, Ranganathan T, Thondiyath A. Computational fluid dynamic study on the effect of winglet addition in flapping hydrofoils to evaluate the propulsive performance of wave gliders. In: OCEANS 2022-Chennai. IEEE; 2022, p. 1–4.
[94] Ntouras D, Papadakis G, Belibassakis K. Ship bow wings with application to trim and resistance control in calm water and in waves. J Marine Sci Eng 2022;10(4):492.
[95] Sang H, Liu G, Sun X, Li C, Wang L, Wang L. Hydrodynamic performance analysis of flapping hydrofoil for single-body architecture wave glider. Ocean Eng 2022;261:112118.
[96] Sang H, Zhang J, Sun X, Li C, Wang L, Wang L. Optimal design and dynamic analysis of hydrofoil mechanism of wave glider. J Marine Sci Eng 2022;10(3):367.
[97] Sun X, Ma S, Sang H, Li C, Liu J. Research on the propulsion performance of spring-hydrofoil mechanism of the wave glider. Ocean Eng 2022;266:112709.
[98] Wang W, Li W, Yan Y, Zhang J. Parametric study on the propulsion and energy harvesting performance of a pitching foil hanging under a wave glider. Renew Energy 2022;184:830–44.
[99] Zhang Y, Xu L, Zhou Y. A wave foil with passive angle of attack adjustment for wave energy extraction for ships. Ocean Eng 2022;246:110627.
[100] Zhang W, Li Y, Liao Y, Jia Q, Pan K. Hydrodynamic analysis of self-propulsion performance of wave-driven catamaran. J Marine Sci Eng 2021;9(11):1221.
[101] Qi Z, Jiang M, Jia L, Zou B, Zhai J. The effect of mass ratio and damping coefficient on the propulsion performance of the semi-active flapping foil of the wave glider. J Marine Sci Eng 2020;8(5):303.
[102] Chang Z, Feng Z, Sun X, Deng C, Zheng Z. Coupled multibody-fluid dynamic analysis for wave glide. In: IFToMM world congress on mechanism and machine science. Springer; 2019, p. 3283–90.
[103] Kumar R, Shin H. Thrust prediction of an active flapping foil in waves using CFD. J Marine Sci Eng 2019;7(11):396.
[104] Wang D, Liu K, Huo P, Qiu S, Ye J, Liang F. Motions of an unmanned catamaran ship with fixed tandem hydrofoils in regular head waves. J Marine Sci Technol 2019;24(3):705–19.
[105] Yang F, Shi W, Zhou X, Guo B, Wang D. Numerical investigation of a wave glider in head seas. Ocean Eng 2018;164:127–38.
[106] Xie H, Wang D, Lin Z, Qiu S, Ye J. Hydrodynamic performance of tandem oscillating foils in waves. In: The 27th international ocean and polar engineering conference. OnePetro; 2017.
[107] Liu P, Su Y-m, Liao Y-l. Numerical and experimental studies on the propulsion performance of a wave glide propulsor. China Ocean Eng 2016;30(3):393–406.
[108] Hao H, Guo Z, Ma Q, Dai S. A preliminary study on the hydrodynamic propulsive force of a pair of inversely oscillating hydrofoils. In: The twenty-fifth international ocean and polar engineering conference. OnePetro; 2015.
[109] Ananthakrishnan P. Hydrodynamic analysis of flapping foils for propulsion of shallow-water and near-surface underwater vehicles. In: International conference on offshore mechanics and arctic engineering. 45493, American Society of Mechanical Engineers; 2014, V007T12A023.
[110] Chiu F-C, Li W-F, Tiao W-C. Preliminary study on a concept of wave propulsion by an active pitch-oscillating fin. In: OCEANS 2014-TAIPEI. IEEE; 2014, p. 1–5.
[111] Li Y, Zhang W, Liao Y, Jia Q, Jiang Q. Multi-energy-system design and experimental research of natural-energy-driven unmanned surface vehicle. Ocean Eng 2021;240:109942.
[112] SEATECH2020. 2020, URL https://seatech2020.eu/. [Accessed on 17 June 2023].
[113] Belibassakis K, Bleuanus S, Vermeiden J, Townsend N. Combined performance of innovative biomimetic ship propulsion system in waves with dual fuel ship engine and application to short-sea shipping. In: The 31st international ocean and polar engineering conference. OnePetro; 2021.
[114] Belibassakis K, Vermeiden J, Öster A. Development and testing of biomimetic dynamic-foil thruster for augmenting ship propulsion in waves. In: OCEANS 2021: San Diego–Porto. IEEE; 2021, p. 1–6.
[115] Belibassakis K, Filippas E, Papadakis G. Numerical and experimental investigation of the performance of dynamic wing for augmenting ship propulsion in head and quartering seas. J Marine Sci Eng 2021;10(1):24.
[116] Ventikos NP, Perera LP, Sotiralis P, Annetis E, Stamatopoulou EV. A life-cycle cost framework for onboard emission reduction technologies: The case of the flapping-foil thruster propulsion innovation. In: International conference on offshore mechanics and arctic engineering, vol. 85895. American Society of Mechanical Engineers; 2022, V05AT06A009.
[117] unknown. Wave power runs model boat. Popular Sci 1935;26.
[118] McCubbin J. Waves serve as boat's engine. Popular Sci 1950;224.
[119] Gause J. Flexible fin propulsion member and vessels incorporated same. In: GB patenet, vol. 1176559. 1966.
[120] Jakobsen E. The foil propeller, wave power for propulsion. In: 2nd International symposium on wave and tidal energy, 1981. BHRA fluid Engineering; 1981, p. 363–9.
[121] Dybdahl K. Foilpropellen kan revolusjonere skipsfarten. Tek Ukebl /Tek 1988;39:10–1.
[122] Lopes D, de Campos JF, Sarmento A, Vaz G. Semi-empirical model study of propulsion with in-line tandem flapping hydrofoils. In: Developments in renewable energies offshore. CRC Press; 2020, p. 746–54.
[123] Jemt T. Propulsion device for propelling a floating watercraft, a conversion kit for replacing a propeller where the kit comprises such a propulsion device, a watercraft comprising such a propulsion device and a method for increasing the efficiency by using such a conversion kit. In: Google patents. 2014, US Patent 8, 684, 777, URL https://patentimages.storage.googleapis.com/61/13/a6/246e786677dba8/US8684777.pdf.
[124] Kumar R, Shin H. Thrust estimation of a flapping foil attached to an elastic plate using multiple regression analysis. Int J Naval Archit Ocean Eng 2019;11(2):828–34.
[125] Kumar R, Shin H. Modified thrust empirical formula of a flapping foil by including the effects of azimuth angles. Int J Naval Archit Ocean Eng 2021;13:126–35.
[126] Bøckmann E, Yrke A, Steen S. Fuel savings for a general cargo ship employing retractable bow foils. Appl Ocean Res 2018;76:1–10.
[127] Bowker JA. Coupled dynamics of a flapping foil wave powered vessel [Ph.D. thesis], University of Southampton; 2018.
[128] Li C, Sang H, Sun X, Qi Z. Hydrographic and meteorological observation demonstration with wave glider "black pearl". In: Intelligent robotics and applications: 10th international conference, ICIRA 2017, Wuhan, China, August 16–18, 2017, Proceedings, Part I 10. Springer; 2017, p. 790–800.
[129] Siddle E, Heywood KJ, Webber BG, Bromley P. First measurements of ocean and atmosphere in the T ropical N orth A tlantic using C aravela, a novel uncrewed surface vessel. Weather 2021;76(6):200–4.
[130] Arredondo-Galeana A, Shi W, Olbert G, Scharf M, Ermakov A, Ringwood J, et al. A methodology for the structural design of LiftWEC: A wave-bladed cyclorotor. In: Proceedings of the 14th European wave and tidal energy conference 27th Aug-1st Sept 2017. European Wave and Tidal Energy Conference; 2021, 1967–1.
[131] Siegel SG. Numerical benchmarking study of a cycloidal wave energy converter. Renew Energy 2019;134:390–405.